People's Democratic Republic of Algeria

Ministry of Higher Education and Scientific Research

University M'Hamed BOUGARA - Boumerdes

Institute of Electrical and Electronic Engineering

Department of Electronics

Final Year Project Report Presented in Partial Fulfillment of the Requirements for the Degree of

MASTER

In **Power Engineering**

Option: **Power Engineering**

Title

Optimal Power System Stabilizers design via PSO algorithm

Presented by:

- DJELLAL Mohamed Riadh

- BENREKIA Mohamed

Supervisor:

Pr. A. Kheldoun

Abstract

Power system stabilizers (PSSs) form an essential part of power systems. Their main function is to enhance the system's stability. The classical PSSs are no longer helpful in order to achieve the stability of the system in an optimal way. This introduces the idea of optimal tuning of PSS parameters in order to find the best parameters. Several optimization techniques are used to achieve such a goal, one of them is the Particle Swarm Optimization (PSO) algorithm. The two-area four-machine power system is simulated in Simulink MATLAB and studied in different scenarios. At first, simulation is done without a PSS, then the system is supported with a classical PSS. After that, the PSO algorithm is introduced to the system in order to find the optimal PSS parameters. Two objective functions are investigated, one is time domain based and the other one is eigenvalues based. Each simulation is provided with its eigenvalues calculation in order to show how much the system has become stable.

Dedication

Every challenging work needs self -efforts as well as guidance of elders especially those who were very close to our heart. I dedicate this work to:

***The soul of my grandfather**,*

***GHOUL MAAMAR** who passed away on 11/09/2021*

For being my first teacher.

إنا لله وإنا إليه راجعون

My beloved father and mother,

Whose affection, love, encouragement and prays of day and night make me able to get such success and honor.

My sisters and my family,

Who shared their words of advice and encouragement to finish this work.

My friends,

Who have supported me throughout the process. I will always appreciate all they have done.

DJELLAL Mohamed Riadh

Dedication

I would like to dedicate this work to:

***My parents**, I hope that this achievement will complete the dream that you had for me all those many years ago when you chose to give me the best education you could.*

***My brothers and sisters**, who shared their words of advice and encouragement to finish this work.*

***My friends**, who mean the world to me. I'm more than thankful to all of their support and encouragement during the time I needed them the most.*

Mohamed BENREKIA

Acknowledgments

First and foremost, Alhamdulillah, all praises and thanks to Allah Who provided us confidence, guidance & strength to complete this work.

Our deep gratitude and thanks go to our supervisor **Pr. A. Kheldoun** for devoting much time to supporting us through the completion of our work. His special interest and knowledge in issues related to power systems enabled him to give us the right guidance and also provided us with much needed motivation.

We acknowledge with much appreciation the jury members for having honored us by agreeing to evaluate this work.

Finally, we express our sincere thanks to the teaching faculty who helped us directly and indirectly in the completion of this task successfully.

Table of Contents

List of Tables

List of figures

General Introduction

Modern power systems are the most complex human-made engineering systems, which significantly change human life and society development. A power system is defined as the electric power sources, conductors, and equipment required to supply electric power. The overall system is made up of several generating sources and several layers of transmission networks. The main function of a power system is to convert energy from its natural form to electrical form and transport it to consumers. The energy demand has to be met at any instant in time by corresponding generation. Several challenges are facing the power system when trying to meet the changing load demand, one example is the constancy of the voltage and frequency over the whole system, this is must be achieved in a reliable way.

Power systems are usually subjected to different kinds of disturbances that may affect the normal operation of the system. These disturbances can be large or small and can occur in many forms, like: loss of synchronism between the generating units of the system, load changes, short-circuits and faults, loss of a large generator or load, …etc. The system must be able to operate properly in normal conditions, and also to regain the state of stability when subjected to these kinds of disturbances. This introduces the concept of Power System Stability.

Power system stability is classified into three main types: frequency stability, voltage stability, and rotor angle stability. Rotor angle stability refers to the ability of synchronous generators of an interconnected power system to remain in synchronism after being subjected to disturbance. It has two main types: large-disturbance rotor angle stability (transient stability), or small-signal rotor angle stability; the main focus for this study.

Small signal stability is the ability of the power system to maintain synchronism when subjected to small disturbances. Power System Stabilizers (PSS) are added to the system in order to achieve this kind of stability. Classical PSSs (CPSS) are now routinely used to damp out low frequency oscillations by controlling the excitation system of the generator using auxiliary stabilizing signals. The problem with CPSSs is that they give poor performance under varying operating conditions, because the power system is highly nonlinear and its parameters vary all the time. This introduces the idea to tune the PSS parameters in order to achieve high effectiveness in stability.

Several optimization techniques are used to perform the optimization of power system stabilizers. One technique is Particle Swarm Optimization algorithm (PSO), the tuning of the PSS parameters is converted to a constrained optimization problem. After setting the ground for the PSO algorithm, it will produce the best suitable PSS parameters. This is done via two objective functions, the first is time domain based and the other one is eigenvalues based.

The system used for this study is the two-area four-machine power system, its data are taken from reference [1]. The system is simulated in Simulink MATLAB and tested in different scenarios. At first, the two area four machine system is simulated with no PSS. Then the simulation is done including the classical PSS from Kundur book (reference [1]). At the end, the PSO algorithm is introduced to the system with two different objective functions and new PSS parameters will result. For each case, the eigenvalues of the system are calculated in order to measure the robustness of system stability. Because the eigenvalues of a system reflect how much it is stable.

This work is divided to three chapters:

* The first chapter is about power system modeling. Since the system's modeling is very important in the stability studies, the models of all power systems components are presented in this chapter.

* The second chapter deals with stability and its types, it emphases mainly on the analysis of small-signal rotor angle stability since it is the main focus for this study.

* The third chapter is about particle swarm optimization algorithm and how it is fitted to the system model in order to optimize the PSS parameters. It shows also the simulation results of the different scenarios as discussed before.

Chapter I

Power System Modeling

Chapter I: Power System Modeling

1.1 Introduction

The most complex systems ever developed by man are power systems. The inclusion of numerous devices, both in terms of transmission and generation sources, has made the modern power grid more sophisticated. The primary role of an electric power system is to transform energy from one of the naturally accessible forms to electrical form, because of its ease of transportation and its high flexibility, and transfer it to the points of use. Energy is rarely utilized in its electrical form but rather converted to various forms, such as heat, light, and mechanical energy. In order for a power system to operate properly, it must meet some requirements which are:

1) The system must be able to meet the continually changing load demand for active and reactive power.
2) The system should supply energy at minimum cost and with minimum ecological impact.
3) Constancy of frequency and voltage must be achieved while certain level of reliability must be satisfied too[1]

An electrical power system is made up of several separate parts that are linked together to produce a vast, sophisticated, and dynamic system capable of generating, transmitting, and distributing electrical energy across a broad region. Therefore, a power system is divided into four main stages, which are: Generation, Transmission and Sub-transmission, Distribution, and Loads.

1.2 Structure of power systems

The basic structure of modern-day power system is shown in Fig.1.1. A power system is usually divided into four parts: Generation, Transmission and Sub-transmission, Distribution, and Loads.

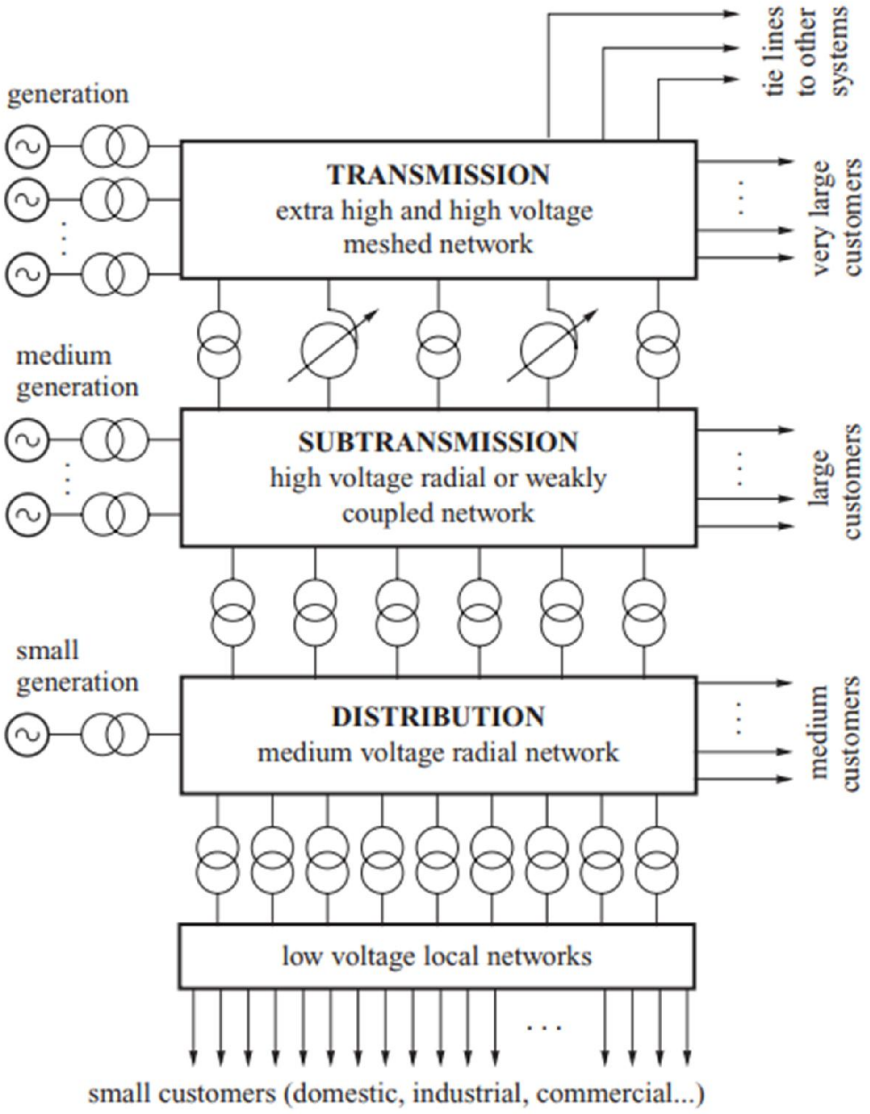

Fig. 1.1 Structure of Power System

1.2.1 Generation

In generating stations, the fuel (coal, water, nuclear energy, etc.) is converted into electrical energy. The electrical power is generated in the range of 11kV to 25kV, which is then stepped-up for long distance transmission. The conversion of mechanical to electrical energy in traditional thermal or hydro plants is almost universally achieved by the use of a synchronous generator. The synchronous generator feeds its electrical power into the transmission system via a step-up transformer in order to increase the voltage from the generation level to the transmission level (hundreds of kilovolts). [3] [4]

1.2.2 Transmission and Sub-transmission:

The transmission substation carries the overhead lines which transfer the generated electrical energy from generation to the distribution substations. Transmission lines also interconnect neighboring utilities which permits not only economic dispatch of power within regions during normal conditions, but also the transfer of power between regions during emergencies. The portion of the transmission system that connects the high-voltage substation through step-down transformers to the distribution substations are called the *sub-transmission* network [5]. Some large industrial customers may be served from this system directly [2].

1.2.3 Distribution:

The distribution system is the part which connects the distribution substations to the consumers which can be domestic, commercial and relatively small consumers. They are designed to supply continuous and reliable power at the consumers' terminals at minimum cost.

1.2.4 Loads

The demand for electrical power is never constant and changes continuously throughout the day and night. The changes in demand of individual consumers may be fast and frequent, but as one moves up the power system structure from individual consumers, through the distribution network, to the transmission level, the changes in demand become smaller and smoother as individual demands are aggregated. Consequently, the total power demand at the transmission level changes in a more or less predictable way that depends on the season, weather conditions, way of life of a particular society, and so on [3].

1.3 Power system model

The first step in analyzing and controlling an electrical power system is to find a "good" mathematical model. Generally, a model is a set of equations or relations, which suitably describes the interactions between the different variables studied, in the time range considered and with the desired precision, for an element or a system.

In many cases, choosing the correct model is often the most difficult part of the study. The essential point is to find the "good model" which achieves a compromise between the accuracy of the qualitative and quantitative behavior and the simplicity of implementation for purposes of analysis and synthesis [6].

The models of synchronous generator, excitation system, prime mover, transmission lines, loads, and power system stabilizer are presented in the following.

1.3.1 Synchronous Generators

The synchronous generators are the main source of the electrical energy in power systems. They are at the heart of any power system, therefor, a necessary condition for a system to operate properly is that all synchronous machines remain in synchronism (in step) [1].

Synchronous generator consists of two parts rotor and stator. The rotor part consists of field windings and stator part consists of armature conductors. The field winding is excited by direct current. The rotation of field poles in the presence of armature conductors induces an alternating voltage which results in electrical power generation [7]. The frequency of the stator electrical quantities is thus synchronized with the rotor mechanical speed: hence the designation "synchronous machine". [1]

As shown in Fig 1.2, the armature windings which are located on stator, are the three phase windings (a, b, c) which are distributed 120° apart in space so that, with uniform rotation of the magnetic field, voltages displaced by 120° in time phase will be produced in the windings [1]. Whereas, the four windings on the rotor are:

* The field winding connected to the exciter (*fd*).

* The d-axis damper (*1d*):

    d: direct axis, which is a spinning axis directly in line with the "north pole" of the field winding.

* Two q-axis dampers (*1q, 2q*):

    q: quadrature axis, which is a spinning axis 90 degrees out of phase with the d-axis.

The damper windings (d and q axis dampers); also called amortisseur windings, are extra windings that provide start-up torque and damping for the machine, they also create a force that attempt to bring the machine to 60Hz or 50 Hz [9]. Some conventions are made in order to proceed the modeling are: q-axis leads the d-axis and the rotor angle Θ_{shaft} is the angle between phase a-axis and q-axis and all equations will be written for a p-pole machine (because different sources make different conventions). The equations of the model presented in this chapter are quoted from Saur and Pai book [10].

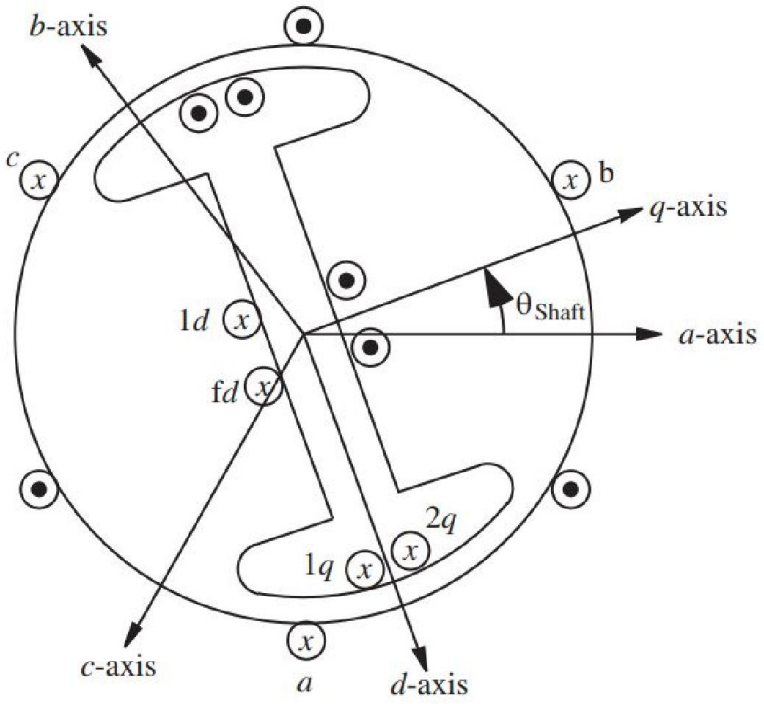

Fig. 1.2 Synchronous generator schematic

Application of fundamental Kirchhoff's, Faraday's and Newton's laws give the following equations for the stator, the rotor, and the shaft:

Stator:

$$v_a = i_a\, r_s + \frac{d\,\lambda_a}{dt} \quad (1.1)$$

$$v_b = i_b\, r_s + \frac{d\,\lambda_b}{dt} \quad (1.2)$$

$$v_c = i_c\, r_s + \frac{d\,\lambda_c}{dt} \quad (1.3)$$

Rotor:

$$v_{fd} = i_{fd}\, r_{fd} + \frac{d\,\lambda_{fd}}{dt} \quad (1.4)$$

$$v_{1d} = i_{1d}\, r_{1d} + \frac{d\,\lambda_{1d}}{dt} \quad (1.5)$$

$$v_{1q} = i_{1q}\, r_{1q} + \frac{d\,\lambda_{1q}}{dt} \quad (1.6)$$

$$v_{2q} = i_{2q}\, r_{2q} + \frac{d\,\lambda_{2q}}{dt} \quad (1.7)$$

Shaft:

$$\frac{d\,\Theta_{shaft}}{dt} = \frac{2}{P}\,\mathrm{w} \quad (1.8)$$

$$\mathrm{J}\,\frac{2}{P}\,\frac{d\mathrm{w}}{dt} = T_m - T_e - T_{fw} \quad (1.9)$$

Where λ is flux linkage, r is winding resistance, J is the inertia constant, P is the number of magnetic poles per phase, T_m is the mechanical torque applied to the shaft, T_e is the torque of electrical origin, and T_{fw} is a friction-windage torque.

Special transformations are done to transform the *abc* phase quantities into another reference frame Called the *dq0 transformation*. The transformation is very similar to that of symmetrical components when dealing with fault analysis [9].

$$\mathrm{V_{dq0}} = \begin{bmatrix} Vd \\ Vq \\ V0 \end{bmatrix} = \mathrm{T_{dq0}}\,\mathrm{V_{abc}} = \mathrm{T_{dq0}} \begin{bmatrix} Va \\ Vb \\ Vc \end{bmatrix} \quad (1.10)$$

$$\mathrm{V_{abc}} = \begin{bmatrix} Va \\ Vb \\ Vc \end{bmatrix} = \mathrm{T_{dq0}^{-1}}\,\mathrm{V_{dq0}} = \mathrm{T_{dq0}^{-1}} \begin{bmatrix} Vd \\ Vq \\ V0 \end{bmatrix} \quad (1.11)$$

The same is applied for the current *i* and for the flux λ.

The matrix T_{dq0} defined as:

$$T_{dq0} \triangleq \frac{2}{3}\begin{bmatrix} \sin\frac{P}{2}\Theta_{shaft} & \sin(\frac{P}{2}\Theta_{shaft} - \frac{2\pi}{3}) & \sin(\frac{P}{2}\Theta_{shaft} + \frac{2\pi}{3}) \\ \cos\frac{P}{2}\Theta_{shaft} & \cos(\frac{P}{2}\Theta_{shaft} - \frac{2\pi}{3}) & \cos(\frac{P}{2}\Theta_{shaft} + \frac{2\pi}{3}) \\ \frac{1}{2} & \frac{1}{2} & \frac{1}{2} \end{bmatrix} \quad (1.12)$$

The inverse T_{dq0}^{-1} is then calculated:

$$T_{dq0}{}^{-1} = \begin{bmatrix} \sin\frac{P}{2}\Theta_{shaft} & \cos\frac{P}{2}\Theta_{shaft} & 1 \\ \sin(\frac{P}{2}\Theta_{shaft} - \frac{2\pi}{3}) & \cos(\frac{P}{2}\Theta_{shaft} - \frac{2\pi}{3}) & 1 \\ \sin(\frac{P}{2}\Theta_{shaft} + \frac{2\pi}{3}) & \cos(\frac{P}{2}\Theta_{shaft} + \frac{2\pi}{3}) & 1 \end{bmatrix} \quad (1.13)$$

After evaluation, the system in *dq0* coordinates has the form:

Stator:

$$v_d = r_s\, i_d - w\lambda_q + \frac{d\,\lambda_d}{dt} \quad (1.14)$$

$$v_q = r_s\, i_q + w\lambda_d + \frac{d\,\lambda_q}{dt} \quad (1.15)$$

$$v_0 = r_s\, i_0 + \frac{d\,\lambda_0}{dt} \quad (1.16)$$

Rotor:

$$v_{fd} = r_{fd}\, i_{fd} + \frac{d\,\lambda_{fd}}{dt} \quad (1.17)$$

$$v_{1d} = r_{1d} i_{1d} + \frac{d\,\lambda_{1d}}{dt} \quad (1.18)$$

$$v_{1q} = r_{1q}\, i_{1q} + \frac{d\,\lambda_{1q}}{dt} \quad (1.19)$$

$$v_{2q} = r_{2q}\, i_{2q} + \frac{d\,\lambda_{2q}}{dt} \quad (1.20)$$

Shaft:

$$\frac{d\,\Theta_{shaft}}{dt} = \frac{2}{P}\,\mathrm{w} \quad (1.21)$$

$$\mathrm{J}\,\frac{2}{P}\,\frac{d\mathrm{w}}{dt} = T_m - T_e - T_{fw} \quad (1.22)$$

The expression of T_e is derived after considering the overall energy or power balance for the machine. This is an electromechanical system that can be divided into an electrical system, a mechanical system, and a coupling field [10]. Fig 1.3 shows a diagram for such power balance for a single machine.

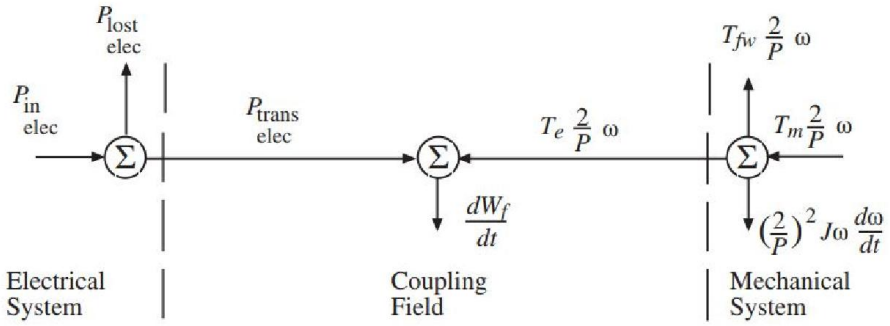

Fig. 1.3 Synchronous machine power balance

The expression of electrical torque T_e is derived after considering that the electrical system losses are in the form of resistance and the mechanical system losses are in the form of friction. The coupling field is assumed to be lossless, hence the movement of energy between the electrical and mechanical systems can be tracked easily [9].

$$T_{elec} = -\frac{3}{2}\frac{P}{2}(\lambda_d I_q - \lambda_q I_d) \qquad (1.23)$$

To complete the dynamic model in the transformed variables it desirable to define an angle that is constant for constant shaft speed. It is defined as follows [10]:

$$\delta \triangleq \frac{P}{2}\Theta_{shaft} - w_s t \qquad (1.24)$$

where ω_s is a constant normally called rated synchronous speed in electrical radians per second, giving:

$$\frac{d\delta}{dt} = w - w_s \qquad (1.25)$$

and $$\mathrm{J}\frac{2}{P}\frac{dw}{dt} = T_m + \frac{3}{2}\frac{P}{2}(\lambda_d i_q - \lambda_q i_d) - T_{fw} \qquad (1.26)$$

The model of the per-unitized equations is presented as follows (keeping in mind that the coupling field is assumed to be lossless):

Mechanical dynamic equations:

$$\frac{d\delta}{dt} = \Delta w_{pu} * w_s \qquad (1.27)$$

$$2H\frac{dw}{dt} = \frac{P_{mech}}{1+\Delta w_{pu}} - (\psi_d I_q - \psi_q I_d) \qquad (1.28)$$

Stator dynamic equations:

$$\frac{1}{w_s}\frac{d\psi_d}{dt} = R_s I_d + (1 + \Delta w_{pu})\psi_q + V_{dterm} \qquad (1.29)$$

$$\frac{1}{w_s}\frac{d\psi_q}{dt} = R_s I_q - (1 + \Delta w_{pu})\psi_d + V_{qterm} \qquad (1.30)$$

$$\frac{1}{w_s}\frac{d\psi_0}{dt} = R_s I_0 + V_{0term} \qquad (1.31)$$

Rotor dynamic equations:

$$T'_{d0}\frac{dE'_q}{dt} = E_{fd} - E'_q - (X_d - X'_d)\left(I_d - \frac{X'_d - X''_d}{(X'_d - X_l)^2}(+\psi'_d + (X'_d - X_l)I_d - E'_q)\right) \qquad (1.32)$$

$$T'_{q0}\frac{dE'_d}{dt} = -E'_d - (X_q - X'_q)\left(I_q - \frac{X'_q - X''_q}{(X'_q - X_l)^2}(-\psi'_q + (X'_q - X_l)I_q - E'_d)\right) \qquad (1.33)$$

$$T''_{d0}\frac{d\psi'_d}{dt} = -\psi'_d - (X'_d - X_l)I_d + E'_q \qquad (1.34)$$

$$T''_{q0}\frac{d\psi'_q}{dt} = -\psi'_q - (X'_q - X_l)I_q + E'_d \qquad (1.35)$$

Algebraic relationship between stator and rotor fluxes:

$$\psi_d = -I_d X''_d + E'_q\frac{X''_d - X_l}{X'_d - X_l} + \psi'_d\frac{X'_d - X''_d}{X'_d - X_l} \qquad (1.36)$$

$$\psi_q = -I_q X''_q + E'_d\frac{X''_q - X_l}{X'_q - X_l} + \psi'_q\frac{X'_q - X''_q}{X'_q - X_l} \qquad (1.37)$$

Where:

w_s: is the synchronous speed ($2\pi f$).

Δw_{pu}: is the deviation of rotor speed away from synchronous speed.

I_d, I_q, I_0: are the stator current in dq0 reference.

V_{dterm}, V_{qterm}, V_{0term}: are the stator voltage in the dq0 reference.

Ψ_d, Ψ_q, Ψ_0: are the stator flux in the dq0 reference.

E'_d, E'_q, Ψ'_q, Ψ'_d: are the per-unitized versions of the rotor voltages and fluxes.

E_{fd}: the field voltage input (from the exciter).

P_{mech}: the mechanical power input from turbine/governor.

H: inertia constant in sec.

R_S: armature resistance in pu.

X_l: armature leakage reactance in pu.

X_d: synchronous reactance along the d-axis in pu.

X'_d: transient reactance along the d-axis in pu.

X''_d: sub-transient reactance along the d-axis in pu.

X_q: synchronous reactance along the q-axis in pu.

X'_q: transient reactance along the q-axis in pu.

X''_q: sub-transient reactance along the q-axis in pu.

T'_{d0}: d-axis open circuit transient time constant in sec.

T''_{d0}: d-axis open circuit sub-transient time constant in sec.

T'_{q0}: q-axis open circuit transient time constant in sec.

T''_{q0}: q-axis open circuit sub-transient time constant in sec.

In the stator differential equations, regardless of what the derivative of these fluxes are, they are multiplied by a very small number ($\frac{1}{w_s}$) and thus the left-hand side is near zero anyway, so an approximation is made:

$$\frac{1}{w_s}\frac{d\psi_d}{dt} \approx 0 = R_s I_d + \left(1 + \Delta w_{pu}\right)\psi_q + V_{dterm} \qquad (1.38)$$

$$\frac{1}{w_s}\frac{d\psi_q}{dt} \approx 0 = R_s I_q - \left(1 + \Delta w_{pu}\right)\psi_d + V_{qterm} \qquad (1.39)$$

$$\frac{1}{w_s}\frac{d\psi_0}{dt} \approx 0 = R_s I_0 + V_{0term} \qquad (1.40)$$

This gives the following:

$$V_{dterm} = -R_s I_d - \left(1 + \Delta w_{pu}\right)\psi_q \qquad (1.41)$$

$$V_{qterm} = -R_s I_q + \left(1 + \Delta w_{pu}\right)\psi_d \qquad (1.42)$$

Replacing equations (1.37) and (1.36) in equations (1.41) and (1.42) respectively gives:

$$V_{dterm} = -R_s I_d - \left(1 + \Delta w_{pu}\right)\left(-I_q X"_q + E'_d \frac{X"_q - X_l}{X'_q - X_l} + \psi'_q \frac{X'_q - X"_q}{X'_q - X_l}\right) \quad (1.43)$$

$$V_{qterm} = -R_s I_q + \left(1 + \Delta w_{pu}\right)\left(-I_d X"_d + E'_q \frac{X"_d - X_l}{X'_d - X_l} + \psi'_d \frac{X'_d - X"_d}{X'_d - X_l}\right) \quad (1.44)$$

This implies:

$$V_{dterm} = -R_s I_d + \left(1 + \Delta w_{pu}\right) I_q X"_q + \left(1 + \Delta w_{pu}\right)\left(+E'_d \frac{X"_q - X_l}{X'_q - X_l} + \psi'_q \frac{X'_q - X"_q}{X'_q - X_l}\right) \quad (1.45)$$

$$V_{qterm} = -R_s I_q - \left(1 + \Delta w_{pu}\right) I_d X"_d + \left(1 + \Delta w_{pu}\right)\left(+E'_q \frac{X"_d - X_l}{X'_d - X_l} + \psi'_d \frac{X'_d - X"_d}{X'_d - X_l}\right) \quad (1.46)$$

Setting:

$$E"_d = +E'_d \frac{X"_q - X_l}{X'_q - X_l} + \psi'_q \frac{X'_q - X"_q}{X'_q - X_l} \quad (1.47)$$

$$E"_q = +E'_q \frac{X"_d - X_l}{X'_d - X_l} + \psi'_d \frac{X'_d - X"_d}{X'_d - X_l} \quad (1.48)$$

Gives the following:

$$V_{dterm} = -R_s I_d + \left(1 + \Delta w_{pu}\right) I_q X"_q + \left(1 + \Delta w_{pu}\right) E"_d \quad (1.49)$$

$$V_{qterm} = -R_s I_q - \left(1 + \Delta w_{pu}\right) I_d X"_d + \left(1 + \Delta w_{pu}\right) E"_q \quad (1.50)$$

The term $(1+\Delta w_{pu})$ is removed because multiplying all the transmission line X values by per unit frequency to scale the network impedances as system frequency changes cannot be done in stability studies [9].

$$V_{dterm} = E^{"}{}_{d}\left(1 + \Delta w_{pu}\right) - R_s I_d + I_q X"_q \qquad (1.51)$$

$$V_{qterm} = E^{"}{}_{q}\left(1 + \Delta w_{pu}\right) - R_s I_q - I_d X"_d \qquad (1.52)$$

The final complete model of per-unitized equations is:

Algebraic relationships:

$$E^{"}{}_{d} = +E'_d \frac{X^{"}{}_q - X_l}{X'_q - X_l} + \psi'_q \frac{X'_q - X"_q}{X'_q - X_l} \qquad (1.53)$$

$$E^{"}{}_{q} = +E'_q \frac{X^{"}{}_d - X_l}{X'_d - X_l} + \psi'_d \frac{X'_d - X"_d}{X'_d - X_l} \qquad (1.54)$$

$$\psi_d = -I_d X"_d + E^{"}{}_{d} \qquad (1.55)$$

$$\psi_q = -I_q X"_q + E^{"}{}_{q} \qquad (1.56)$$

$$V_{dterm} = E^{"}{}_{d}\left(1 + \Delta w_{pu}\right) - R_s I_d + I_q X"_q \qquad (1.57)$$

$$V_{qterm} = E^{"}{}_{q}\left(1 + \Delta w_{pu}\right) - R_s I_q - I_d X"_d \qquad (1.58)$$

Differential equations:

$$\frac{d\delta}{dt} = \Delta w_{pu} * w_s \qquad (1.59)$$

$$2H \frac{d\mathrm{w}}{dt} = \frac{P_{mech}}{1+\Delta w_{pu}} - (\psi_d I_q - \psi_q I_d) \qquad (1.60)$$

$$T'_{d0} \frac{d E'_q}{dt} = E_{fd} - E'_q - (X_d - X'_d)\left(I_d - \frac{X'_d - X^{"}_d}{(X'_d - X_l)^2}\left(+\psi'_d + (X'_d - X_l) I_d - E'_q\right)\right) \qquad (1.61)$$

$$T'_{q0} \frac{d E'_d}{dt} = -E'_d - \left(X_q - X'_q\right)\left(I_q - \frac{X'_q - X^{"}_q}{\left(X'_q - X_l\right)^2}\left(-\psi'_q + \left(X'_q - X_l\right) I_q - E'_d\right)\right) \qquad (1.62)$$

$$T"_{d0}\ \frac{d\,\psi'_d}{dt} = -\psi'_d - (X'_d - X_l)I_d + E'_q \qquad (1.63)$$

$$T'''_{q0}\ \frac{d\,\psi'_q}{dt} = -\psi'_q - \left(X'_q - X_l\right)I_q + E'_d \qquad (1.64)$$

The field voltage E_{fd} is an input from the exciter. The equation of the product of the field current and the mutual inductance $I_{fd}L_{ad}$ is given as follows:

$$L_{ad}I_{fd} = L'_q + (X_d - X'_d)\left(I_d - \frac{X'_d - X"_d}{(X'_d - X'_l)^2}\left(+\psi'_d + (X'_d - X_l)I_d - E'_q\right)\right) \qquad (1.65)$$

$$T'_{d0}\ \frac{d\,E'_q}{dt} = E_{fd} - L_{ad}I_{fd} \qquad (1.66)$$

Till now, all what have been discussed is about a single machine that is connected to a three-phase system. It is very convenient to transform all synchronous machines stator and network variables into a common reference frame called: the Synchronous Reference Frame (or the network reference frame).

The transformation is done as follows:

$$\begin{bmatrix} V_D \\ V_Q \\ V_0 \end{bmatrix} = T_{sync}V_{abc} = T_{sync}\begin{bmatrix} V_a \\ V_b \\ V_c \end{bmatrix} \qquad (1.67)$$

$$T_{sync} = \frac{2}{3}\begin{bmatrix} cos\, w_s t & cos\,(w_s t - \frac{2\pi}{3}) & cos\,(w_s t + \frac{2\pi}{3}) \\ -sin\, w_s t & -sin\,(w_s t - \frac{2\pi}{3}) & -sin\,(w_s t + \frac{2\pi}{3}) \\ \frac{1}{2} & \frac{1}{2} & \frac{1}{2} \end{bmatrix} \qquad (1.68)$$

$$T_{sync}^{-1} = \frac{2}{3}\begin{bmatrix} cos\, w_s t & -sin\, w_s t & 1 \\ cos\,(w_s t - \frac{2\pi}{3}) & -sin\,(w_s t - \frac{2\pi}{3}) & 1 \\ cos\,(w_s t + \frac{2\pi}{3}) & -sin\,(w_s t + \frac{2\pi}{3}) & 1 \end{bmatrix} \qquad (1.69)$$

$$\text{If } \begin{bmatrix} V_a \\ V_b \\ V_c \end{bmatrix} = \begin{bmatrix} V_t cos\,(w_s t + \alpha) \\ V_t cos\,(w_s t + \alpha - \frac{2\pi}{3}) \\ V_t cos\,(w_s t + \alpha + \frac{2\pi}{3}) \end{bmatrix} \qquad (1.70)$$

is chosen an input for the system, the result is going to be: $\begin{bmatrix} V_D \\ V_Q \\ V_0 \end{bmatrix} = \begin{bmatrix} +V_t cos\,(\alpha) \\ +V_t sin\,(\alpha) \\ 0 \end{bmatrix}$(1.71).

It can be easily remarqued that all the ($w_s t$) terms cancel out. This means that the new reference frame can be treated like a complex number:

$$v_D + jv_Q = V_t \cos(\alpha) + jV_t \sin(\alpha) = V_t e^{j\alpha} \qquad (1.72)$$

The abc quantities are converted to machine reference frame (dq0 reference), there is a need for the dqo quantities to be transformed to the network reference:

$$\begin{bmatrix} V_a \\ V_b \\ V_c \end{bmatrix} = T_{dq0i}^{-1} \begin{bmatrix} V_{di} \\ V_{qi} \\ V_{0i} \end{bmatrix} \qquad (1.73)$$

$$\begin{bmatrix} V_D \\ V_Q \\ V_0 \end{bmatrix} = T_{sync} \begin{bmatrix} V_a \\ V_b \\ V_c \end{bmatrix} = T_{sync} T_{dq0i}^{-1} \begin{bmatrix} V_{di} \\ V_{qi} \\ V_{0i} \end{bmatrix} \qquad (1.74)$$

Therefore, a direct conversion from the machine reference frame into the network reference frame without passing by the abc phase reference.

$$Network\ Reference\ Frame \rightarrow \begin{bmatrix} V_D \\ V_Q \\ V_0 \end{bmatrix} = T_{sync} T_{dq0i}^{-1} \begin{bmatrix} V_{di} \\ V_{qi} \\ V_{0i} \end{bmatrix} \leftarrow Machine\ Reference\ Frame$$

As mentioned in (1.13) and in (1.24) that:

$$T_{dq0}{}^{-1} = \begin{bmatrix} \sin\frac{P}{2}\Theta_{shaft} & \cos\frac{P}{2}\Theta_{shaft} & 1 \\ \sin(\frac{P}{2}\Theta_{shaft} - \frac{2\pi}{3}) & \cos(\frac{P}{2}\Theta_{shaft} - \frac{2\pi}{3}) & 1 \\ \sin(\frac{P}{2}\Theta_{shaft} + \frac{2\pi}{3}) & \cos(\frac{P}{2}\Theta_{shaft} + \frac{2\pi}{3}) & 1 \end{bmatrix} \quad (1.75)$$

and $\delta_i = \frac{P}{2}\Theta_{shaft\,i} - w_s t$ (1.76) which implies that: $\frac{P}{2}\Theta_{shaft\,i} = w_s t + \delta_i$ (1.77)

This makes the inverse matrix $T_{dq0i}{}^{-1}$ for a particular machine "i" looks like the following:

$$T_{dq0i}{}^{-1} = \begin{bmatrix} \sin(w_s t + \delta_i) & \cos(w_s t + \delta_i) & 1 \\ \sin(w_s t + \delta_i - \frac{2\pi}{3}) & \cos(w_s t + \delta_i - \frac{2\pi}{3}) & 1 \\ \sin(w_s t + \delta_i + \frac{2\pi}{3}) & \cos(w_s t + \delta_i + \frac{2\pi}{3}) & 1 \end{bmatrix} \quad (1.78)$$

The matrix multiplication $T_{sync}T_{dq0i}^{-1}$ end up as follows:

$$T_{sync}T_{dq0i}^{-1} = \begin{bmatrix} +\sin(\delta_i) & +\cos(\delta_i) & 0 \\ -\cos(\delta_i) & +\sin(\delta_i) & 0 \\ 0 & 0 & 1 \end{bmatrix} \quad (1.79)$$

The conversion from network to machine reference frame also can be done by the matrix:

$$T_{dq0i}T_{sync}^{-1} = \left(T_{sync}T_{dq0i}^{-1}\right)^{-1} = \begin{bmatrix} +\sin(\delta_i) & -\cos(\delta_i) & 0 \\ +\cos(\delta_i) & +\sin(\delta_i) & 0 \\ 0 & 0 & 1 \end{bmatrix} \quad (1.80)$$

The subscript "i" for all variables and parameters to denote machine i. The final relation between the machine reference frame and the network reference frame, after omitting the zero values will look like this:

$$\begin{bmatrix} V_{dnetwork} \\ V_{qnetwork} \end{bmatrix} = \begin{bmatrix} +\sin(\delta_i) & +\cos(\delta_i) \\ -\cos(\delta_i) & +\sin(\delta_i) \end{bmatrix} \begin{bmatrix} V_{dmachine} \\ V_{qmachine} \end{bmatrix} \quad (1.81)$$

$$\begin{bmatrix} V_{dmachine} \\ V_{qmachine} \end{bmatrix} = \begin{bmatrix} +\sin(\delta_i) & -\cos(\delta_i) \\ +\cos(\delta_i) & +\sin(\delta_i) \end{bmatrix} \begin{bmatrix} V_{dnetwork} \\ V_{qnetwork} \end{bmatrix} \quad (1.82)$$

As a result, the dq values can be treated as real and imaginary numbers and the conversion is then simple complex number rotation:

$$(V_{dnetwork} + jV_{qnetwork}) = (V_{dmachine} + jV_{qmachine})e^{+j(\delta-\frac{\pi}{2})} \quad (1.83)$$

$$(V_{dmachine} + jV_{qmachine}) = (V_{dnetwork} + jV_{qnetwork})e^{-j(\delta-\frac{\pi}{2})} \quad (1.84)$$

The equations that model the connection of the generator to network are

$$V_{dterm} = E^{"}_{d}(1 + \Delta w_{pu}) - R_s I_d + I_q X"_q \quad (1.85)$$

$$V_{qterm} = E^{"}_{q}(1 + \Delta w_{pu}) - R_s I_q - I_d X"_d \quad (1.86)$$

After making the assumption that $X"_q = X"_d$, it gives a simple circuit equation:

$$V_{dterm} + jV_{qterm} = (1 + \Delta w_{pu})(E^{"}_{d} + jE^{"}_{q}) - (R_s + jX"_d)(I_d + jI_q) \quad (1.87)$$

Converting from the "dq" reference to the network reference gives:

$$V_r + jV_i = (1 + \Delta w_{pu})(E^{"}_{d} + jE^{"}_{q})e^{+j(\delta-\frac{\pi}{2})} \quad (1.88)$$

$$I_r + jI_i = (I_d + jI_q)e^{+j(\delta-\frac{\pi}{2})} \quad (1.89)$$

$$V_{rterm} + jV_{iterm} = (V_r + jV_i) - (R_s + jX"_d)(I_r + jI_i) \quad (1.90)$$

1.3.2 Excitation System

The basic function of an excitation system is to provide direct current to the synchronous machine field winding. In addition, the excitation system performs control and protective functions essential to the satisfactory performance of the power system by controlling the field voltage and thereby the field current. [1]

The control functions include the control of voltage and reactive power flow, and the enhancement of system stability. The protective functions ensure that the capability limits of the synchronous machine, excitation system, and other equipment are not exceeded. [1]

There are three distinct types of excitation systems based on the power source for exciter.

1- DC Excitation Systems (DC) which utilize a DC generator with commutator.
2- AC Excitation Systems (AC) which use alternators and either stationary or rotating rectifiers to produce the direct current needed.
3- Static Excitation systems (ST) in which the power is supplied through transformer and rectifiers. [11]

The first two types of exciters are also called rotating exciters which are mounted on the same shaft as the generator and driven by the prime mover. [11]

Fig. 1.4 shows the general functional block diagram of an excitation system (for all the three types defined earlier).

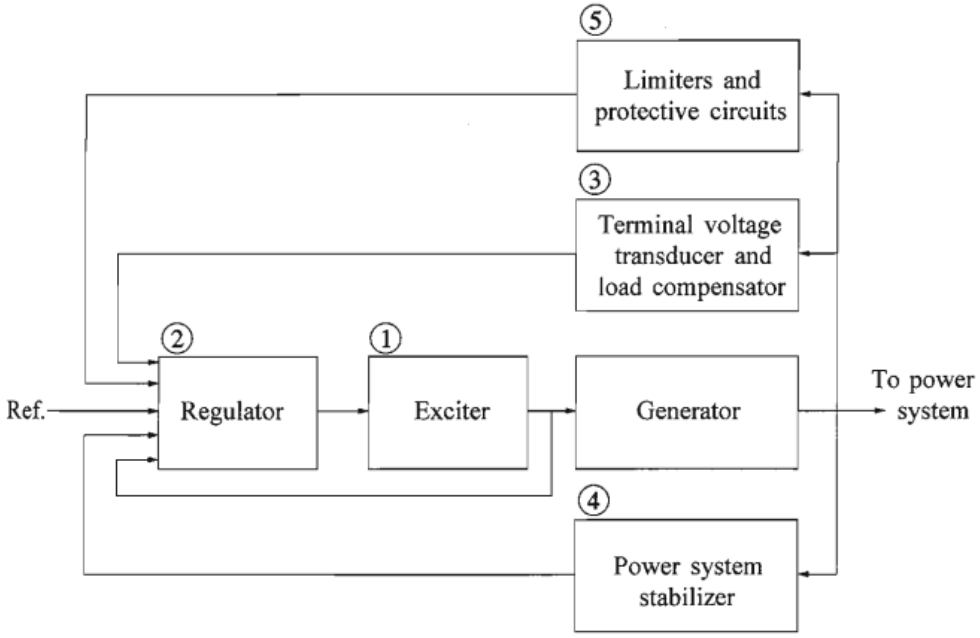

Fig. 1.4 Functional Block Diagram of a Synchronous Generator Excitation Control System

The following is a brief description of the various subsystems identified in Fig. 1.5:

(1) Exciter: provides dc power to the synchronous machine field winding, constituting the power stage of the excitation system. [1]

(2) Regulator: processes and amplifies input control signals to a level and form appropriate for control of the exciter. This includes both regulating and excitation system stabilizing functions. [1]

(3) Terminal voltage transducer and load compensator: senses generator terminal voltage, rectifies and filters it to dc quantity, and compares it with a reference which represents the desired terminal voltage. In addition, load compensation may be provided, if it desired to

hold constant voltage at some point electrically remote from the generator terminal. [1] Its block diagram is shown in Fig. 1.5:

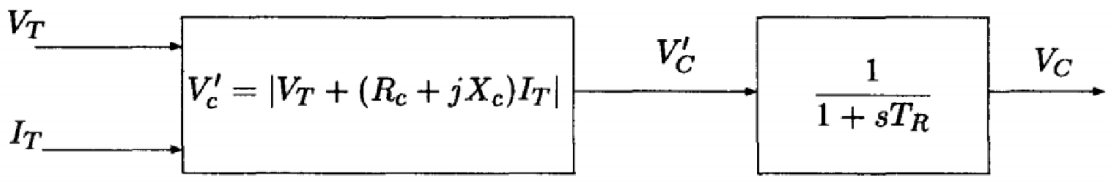

Fig. 1.5 Transducer and load compensator block diagram

(4) Power system stabilizer: provides an additional input signal to the regulator to damp power system oscillations. Some commonly used input signals are rotor speed deviation, accelerating power, and frequency deviation. [1]

(5) Limiters and protective circuits: These include a wide array of control and protective functions which ensure that the capability limits of the exciter and synchronous generator are not exceeded. [1]

One type of the excitation system is the IEEE Type 1 Excitation System is shown in Fig. 1.6.

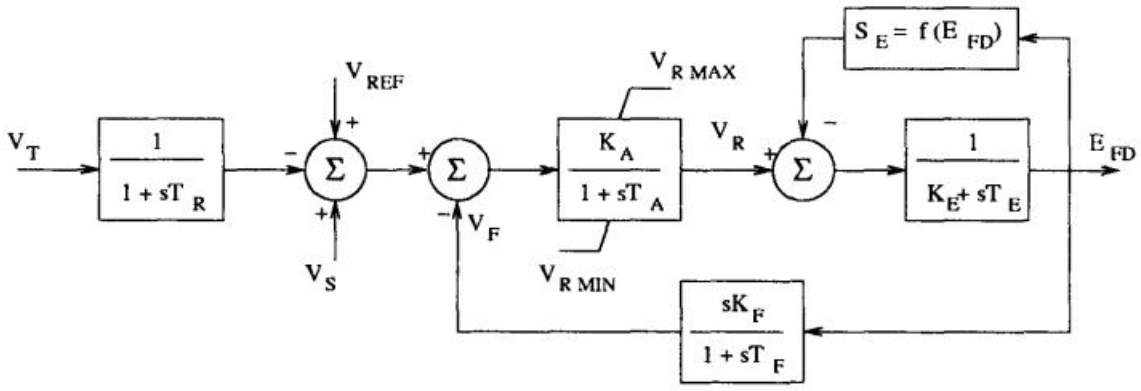

Fig. 1.6 IEEE Type 1 Excitation System

The state equations for the system are given below:

$$\frac{dE_{fd}}{dt} = \frac{1}{T_E}(-[K_E + S_E(E_{FD})]E_{FD} + V_R) \qquad (1.91)$$

$$\frac{dV_2}{dt} = \frac{1}{T_F}\left[-V_2 + \frac{K_F}{T_F}E_{FD}\right] \qquad (1.92)$$

$$\frac{dV_1}{dt} = \frac{1}{T_R}[-V_1 + V_T] \qquad (1.93)$$

$$V_{ERR} = V_{REF} - V_1 \qquad (1.94)$$

$$V_F = \frac{K_F}{T_F}E_{FD} - V_2 \qquad (1.95)$$

$$F_R = \frac{1}{T_A}[-V_R + K_A(V_{ERR} + V_S - V_F)] \qquad (1.96)$$

The limiter of these state equations is a non-windup limiter and is defined as follows:

If $V_R > V_{RMAX}$ set $V_R = V_{RMAX}$

If $V_R = V_{RMAX}$ and $F_R > 0$, set $\frac{dV_R}{dt} = 0$

If $V_R < V_{RMIN}$ set $V_R = V_{RMIN}$

If $V_R = V_{RMIN}$ and $F_R < 0$, set $\frac{dV_R}{dt} = 0$

Otherwise, $\frac{dV_R}{dt} = F_R$

Where:

E_{FD}: Exciter output voltage (applied to generator field) in pu.

T_R: Filter time constant in sec.

K_A: Regulator gain in pu.

T_A: Regulator time constant in sec.

V_{RMIN}: Minimum voltage regulator outputs in pu.

V_{RMAX}: Maximum voltage regulator outputs in pu.

K_E: Exciter constant related to self-excited field in pu.

T_E: Exciter time constant, integration rate associated with exciter control in sec.

K_F: Feedback gain in pu.

T_F: Feedback time constant in sec.

V_T: Generator terminal voltage.

V_R: Regulator output voltage.

S_E: Exciter saturation function.

1.3.3 Prime movers

In a power system, the synchronous generators are normally driven by either steam turbines, or hydro turbines. Each turbine is equipped with a governing system to provide a means by which the turbine can be started, run up to the operating speed and operate on load with the required power output [3]. The power demand from the generator changes corresponding to load characteristics, and the operating conditions of the power system vary continuously. The input mechanical power to the generator must vary in response to these variations to maintain the

frequency constant. Therefore, to regulate the power system frequency, speed control of the prime mover using a governor is required [13].

1.3.3.1 Steam Turbines and their Speed-Governing Systems:

A steam turbine converts stored energy of a high pressure and a high temperature steam into rotating mechanical energy, which is in turn converted into electrical energy by the generator [1]. Steam plants consist of a fuel supply to a steam boiler that supplies a steam chest. The steam chest contains pressurized steam that enters a high-pressure (HP) turbine through a steam valve. The power into the high-pressure turbine is proportional to the valve opening [10]. The governing systems for steam turbines have three basic functions: normal speed/load control, overspeed control, and overspeed trip [1].

1. Speed/Load control: It enables the generating unit to operate satisfactorily in parallel with other units with proper division of load [1].
2. Overspeed control: It is the first line of defense against excessive speed. Its function is to limit the overspeed that occurs on partial or full load rejection and to return the turbine to a steady-state condition such that the turbine is ready for reloading [1].
3. Overspeed trip: or the emergency trip is a backup protection in the event of failure of normal and overspeed control to limit the rotor speed to a safe level [1].

Speed-governing systems of steam turbines can be either Mechanical-Hydraulic or Electro-Hydraulic. Their functional diagrams are presented in the following figures:

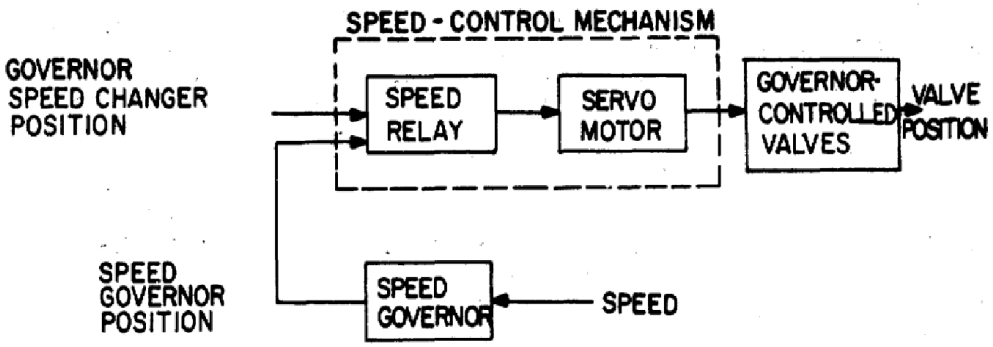

Fig. 1.7 Functional block diagram for mechanical-hydraulic speed-governing systems for steam turbines

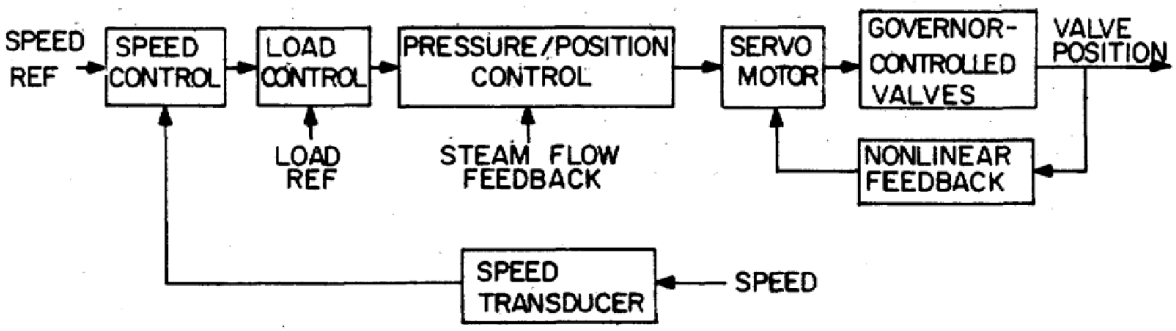

Fig. 1.8 Functional block diagram for electro-hydraulic speed-governing systems for steam turbines

1.3.3.1 Hydro-Turbines and their Speed-Governing Systems:

Hydraulic turbines are the prime movers that convert the energy of the falling water into a rotational mechanical energy and consequently to an electric energy through the use of the generators that are connected to the turbines. Turbines consist of a row of blades that are fixed on a rotating shaft or a plate. The shaft rotates because of the impact of the difference in velocity and pressure of the water striking the blades [14]. The primary basic function of the speed-governing system of the hydro-turbines is to control speed and/or load. The function of speed/load control involves feeding back speed error to control the gate position [1].

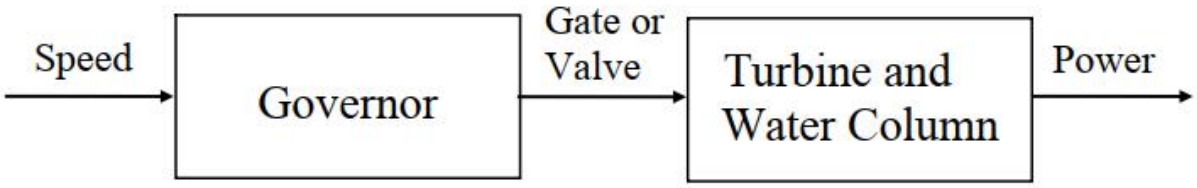

Fig. 1.9 General Governor-Turbine Block Diagram

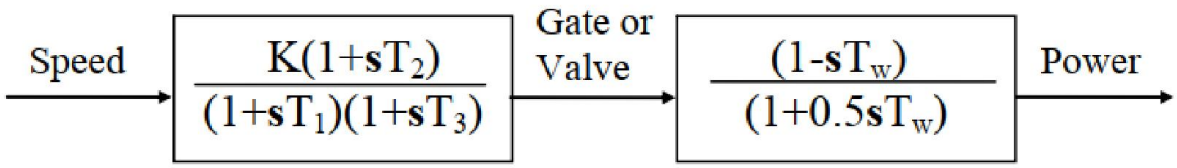

Fig. 1.10 Simple hydro-turbine model.

1.3.4 Loads

In general, to perform power system analysis, models must be developed for all pertinent system components. Inadequate modelling causing under/over-building of the system or degrading reliability between generated power and demand power by loads must be maintained to keep the system continuously in stable operation. Therefore, load characteristics are of crucial importance to be employed in system analysis as they have a significant effect on system performance and highly impact the stability results [13].

Load modeling refers to the mathematical representation of the relationship between the power and voltage in a load bus. Load models can be classified into two main categories: static and dynamic models [15].

A. Static load models

Static models express the active and reactive power at any instant of time as functions of bus voltage magnitudes and frequency [15].

There are two ways of static load representation:

1. Polynomial representation:

Polynomial or ZIP model is commonly used in both steady-state and dynamic studies. This model represents the relationship between the voltage magnitude and power in a polynomial equation that combines constant impedance (Z), current (I), and power (P) components [15].

Both active and reactive power loads are represented by quadratic polynomials given by:

$$\frac{P}{P_0} = a_0 + a_1\left(\frac{V}{V_0}\right) + a_2\left(\frac{V}{V_0}\right)^2 \qquad (1.97)$$

$$\frac{Q}{Q_0} = b_0 + b_1\left(\frac{V}{V_0}\right) + b_2\left(\frac{V}{V_0}\right)^2 \qquad (1.98)$$

Where P_0, Q_0 are initial values of power and reactive power at initial value of voltage V_0. The coefficients a_0, a_1, and a_2 are the fractions of the constant power, constant current and constant impedance components in the active power loads [11].

2. Exponential representation:

It includes not only voltage dependence but also the effect of frequency variations. Active power can be represented as:

$$\frac{P}{P_0} = c_1 \left(\frac{V}{V_0}\right)^{m_{p1}} (1 + k_p \Delta f) + (1 - a_1) \left(\frac{V}{V_0}\right)^{m_{p2}} \qquad (1.99)$$

Where:

c_1: is the frequency dependent fraction of active power load.

m_{p1}: is the voltage exponent for frequency dependent component of active power load.

m_{p2}: is the voltage exponent for frequency independent component of active power load.

Δf: is the per unit frequency deviation.

k_p: is the frequency sensitivity coefficient for the active power load.

The reactive power can be represented as:

$$\frac{Q}{P_0} = c_2 \left(\frac{V}{V_0}\right)^{m_{p1}} (1 + k_{p1} \Delta f) + (\frac{Q_0}{P_0} - c_2) \left(\frac{V}{V_0}\right)^{m_{p2}} (1 + k_{p2} \Delta f) \qquad (1.100)$$

Where:

C_2: is the reactive load coefficient-ratio of initial uncompensated reactive load to total initial active power load P_0.

m_{p1}: is the voltage exponent for the uncompensated reactive load.

m_{p2}: is the voltage exponent for reactive compensation term.

k_{p1}: is the frequency sensitivity coefficient for the uncompensated reactive power load.

k_{p2}: is the frequency sensitivity coefficient for reactive compensation.

B. Dynamic load models:

Static models explained earlier may be accepted for application to composite loads having fast response to voltage/frequency changes and reaching the steady state rapidly. Some cases necessitate considering the dynamics of load components such as discharge lamps, protective relays, thermostatic controlled load, transformers and motors [13]. Not much detail is given to dynamic load modeling because it is not needed in the simulation presented in this report.

1.3.5 Transmission Lines

Electrical power is transferred from generating stations to consumers through transmission lines, which are characterized by four parameters: series resistance R due to the conductor resistivity, shunt conductance G due to leakage current between the phases and ground, series inductance L due to magnetic field surrounding the conductors, and shunt capacitance C due to the electric field between conductors [1].

Transmission lines can be classified according to their lengths as:

1. Short line model:

For lines less than about 80 km (50 miles), the capacitance may be ignored without causing appreciable error in calculating the voltage and current. Therefore, the short line model is obtained by multiplying the series impedance per unit length by the line length.

$$Z = (r + jwL).l = R + jX_L \quad (1.101)$$

Where r and L are respectively the resistance and the inductance per unit of length of the transmission line. l is the line length.

The Figure below shows the short line model on a per-phase basis:

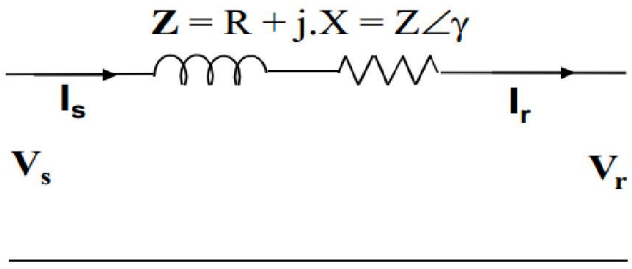

Fig. 1.11 Short length line model

The equations for this model are:

$$Is = Ir \qquad (1.102)$$

$$Vs = Vr + Z.Ir \qquad (1.103)$$

V_s, I_s: are the phase voltage and current at the sending end of the line.

V_r, I_r: are the phase voltage and current at the receiving end of the line.

2. Medium line model:

As the length of the line increases, the line charging current becomes appreciable and the shunt capacitance must be considered. Lines above 80km (50miles) and below 250 km (150miles) in length are termed as medium length lines.

For medium length lines, half of the shunt capacitance may be considered to be lumped at each end of the line. This is referred as the nominal π model as shown in the following figure:

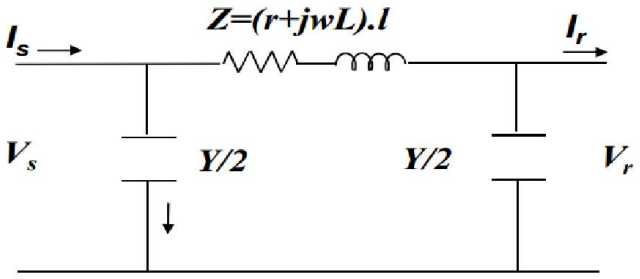

Fig. 1.12 Nominal PI-model of medium length line

Equations for this model are:

$$Is = Y.\left(1 + \frac{ZY}{4}\right).Vr + \left(1 + \frac{ZY}{2}\right).Ir \qquad (1.04)$$

$$Vs = \left(1 + \frac{ZY}{2}\right).Vr + Z.Ir \qquad (1.105)$$

$Y = (g\ + jwC).l = jwcl$ (1.106) as the conductance is neglected g=0.

$$Z = (r\ + jwl).l \qquad (1.107)$$

Where:

C: is the line to neutral capacitance per km

L: is the line inductance per km

l: is the length in km

3. Long line model:

For 250 km (150mile) lines and longer, the effect of distributed parameters must be considered.

The Figure below shows the equivalent PI-circuit of long Transmission line:

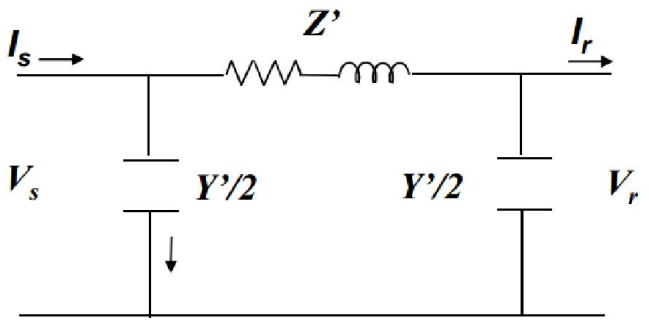

Fig. 1.13 The equivalent PI-circuit of long transmission line

The equations of this model are:

$$Is = Y'.\left(1 + \frac{Z'Y'}{4}\right).Vr + \left(1 + \frac{Z'Y'}{2}\right).Ir \qquad (1.108)$$

$$Vs = \left(1 + \frac{Z'Y'}{2}\right).Vr + Z'.Ir \qquad (1.109)$$

Where

$$Z' = Z.\frac{\tanh \gamma l}{\gamma l} \qquad (1.110)$$

$$Y' = Y.\frac{tanh\frac{\gamma l}{2}}{\frac{\gamma l}{2}} \qquad (1.111)$$

γ known as the propagation constant, is a complex expression given by:

$$\gamma = \sqrt{zy} = \sqrt{(r + jwL)(jCw)} \qquad (1.112)$$

1.3.6 Power system stabilizer

The basic function of a power system stabilizer is to extend stability limits by modulating generator excitation to provide damping to the oscillations of synchronous machine rotors relative to one another. Insufficient damping of these oscillations may limit the ability to transmit power [16]. To provide damping, the stabilizer must produce an electrical torque in phase with the rotor speed deviations [1].

The general block diagram of the PSS is presented in Fig. 1.14.

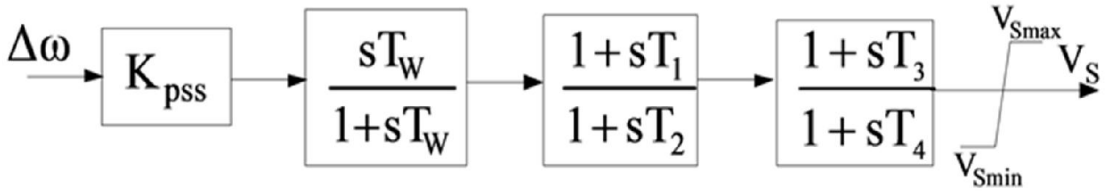

Fig. 1.14 Block diagram of PSS

1.4 Test system

The system used for this study is the two-area four-machine system. It is suitable for study of inter-area oscillations. The one-line diagram of the system is shown in Fig. 1.15. Its data are available in [1].

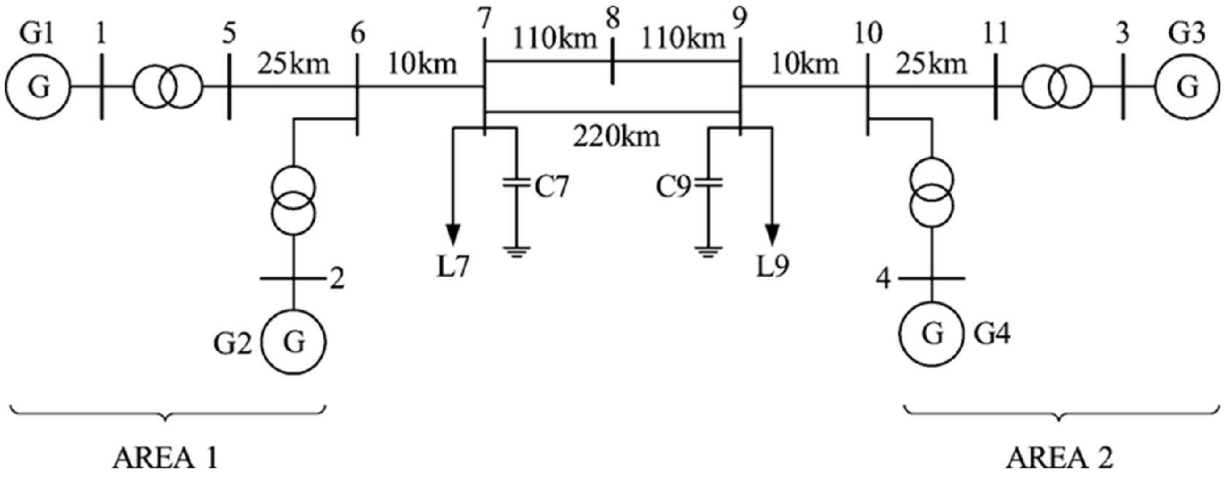

Fig. 1.15 The two-area four-machine power system

1.5 Conclusion

This chapter gives a general overview of power systems. It also explains the different components of power systems along with their models.

Chapter II

Small-signal stability

2.1 Introduction

The power system is a highly nonlinear system that operates in a constantly changing environment; loads, generator outputs and key operating parameters change continually. When subjected to a disturbance, the stability of the system depends on the initial operating condition as well as the nature of the disturbance. Increasingly complex modern power systems require stability analysis, especially for transient and small disturbances [18].

2.2 Definition of power system stability

Power system stability is the ability of an electric power system, for a given initial operating condition, to regain a state of operating equilibrium after being subjected to a physical disturbance, with most system variables bounded so that practically the entire system remains intact [18].

Many major blackouts caused by power system instability have illustrated the importance of this phenomenon [17]. Instability in a power system may be manifested in many different ways depending on the system configuration and operating mode [1].

Maintaining synchronous operation has been a problem for stability. Since power systems rely on synchronous machines for generation of electrical power, a necessary condition for satisfactory system operation is that all synchronous machines remain in synchronism or, colloquially, "*in step*". This aspect of stability is influenced by the dynamics of generator rotor angles and power-angle relationships [1].

2.3 Classification of power system stability

The suggested power system stability categorization is based on the following considerations:

• The physical nature of the resulting instability [1].

• The size of the disturbance considered [1].

• The devices, processes, and time span that must be taken into consideration in order to determine stability [1].

• The most appropriate method of calculation and prediction of stability [1].

The diagram in Fig. 2.1 depicts the overall picture of the power system stability problem, identifying its categories and subcategories. The descriptions of the corresponding forms of stability phenomena are as follows.

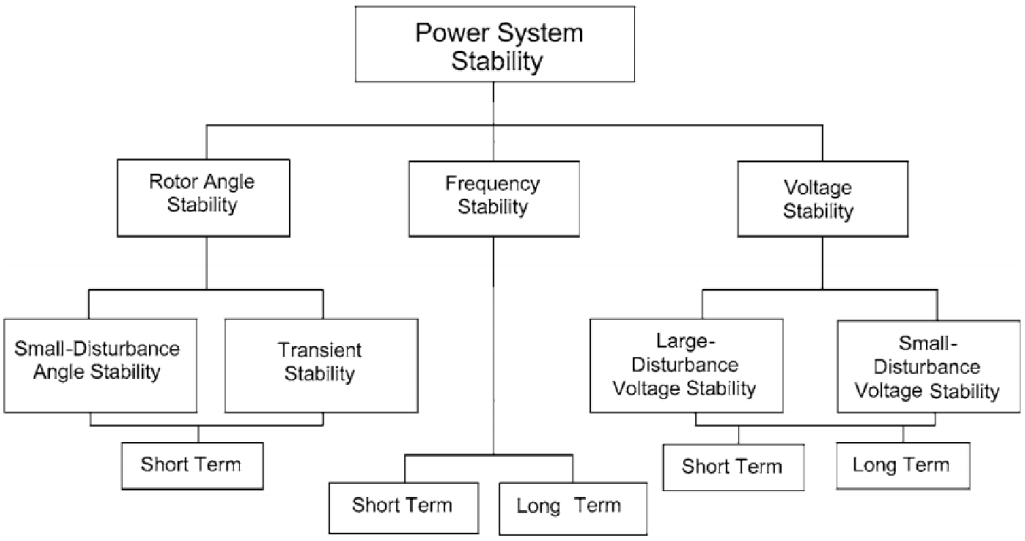

Fig.2.1 Classification of power system stability.

2.3.1 Voltage stability

Voltage stability refers to the ability of a power system to maintain steady voltages at all buses in the system after being subjected to a disturbance from a given initial operating condition. It depends on the ability to maintain/restore equilibrium between load demand and load supply from the power system. Instability that may result occurs in the form of a progressive fall or rise of voltages of some buses. A possible outcome of voltage instability is loss of load in an area or tripping of transmission lines and other elements by their protective systems leading to cascading outages. Loss of synchronism of some generators may result from these outages or from operating conditions that violate field current limit [18].

2.3.2 Frequency stability

Frequency stability refers to the ability of a power system to maintain steady frequency following a severe system upset resulting in a significant imbalance between generation and load. It depends on the ability to maintain/restore equilibrium between system generation and load, with minimum unintentional loss of load. Instability that may result occurs in the form of sustained frequency swings leading to tripping of generating units and/or loads [18].

2.3.3 Rotor angle stability

Rotor angle stability refers to the ability of synchronous machines of an interconnected power system to remain in synchronism after being subjected to a disturbance. It depends on the ability to maintain/restore equilibrium between electromagnetic torque and mechanical torque of each synchronous machine in the system.

Instability that may result occurs in the form of increasing angular swings of some generators leading to their loss of synchronism with other generators [18].

In power systems the power exchange is related the generators rotor angles. Under steady state conditions the equilibrium between the mechanical torque and the electromagnetic torque is maintained and the rotor speed is constant. However, if the system is perturbed the electromagnetic output torque will vary as function of the rotor speed deviation and the rotor angle deviation.

$$\Delta T_e = T_S \Delta\delta + T_D \Delta w \qquad (2.1)$$

Where

$T_S \Delta\delta$: is the component of torque change in phase with the rotor angle perturbation $\Delta\delta$ and is referred to as the synchronizing torque component; T_S is the synchronizing torque coefficient.

$T_D \Delta w$: is the component of torque in phase with the speed deviation Δw and is referred to as the damping torque component; T_D is the damping torque coefficient.

It is usual to characterize the rotor angle stability phenomena in terms of the following two categories:

2.3.3.1 Large-disturbance rotor angle stability (transient stability)

Large-disturbance rotor angle stability or transient stability, as it is commonly referred to, is concerned with the ability of the power system to maintain synchronism when subjected to a severe disturbance, such as a short circuit on a transmission line. The

resulting system response involves large excursions of generator rotor angles and is influenced by the nonlinear power angle relationship [19].

Transient stability depends on both the initial operating state of the system and the severity of the disturbance. Instability is usually in the form of aperiodic angular separation due to insufficient synchronizing torque, manifesting as first swing instability. However, in large power systems, transient instability may not always occur as first swing instability associated with a single mode; it could be a result of superposition of a slow inter-area swing mode and a local-plant swing mode causing a large excursion of rotor angle beyond the first swing. It could also be a result of nonlinear effects affecting a single mode causing instability beyond the first swing [19].

The time frame of interest in transient stability studies is usually 3 to 5 seconds following the disturbance. It may extend to 10–20 seconds for very large systems with dominant inter-area swings [19].

2.3.3.2 Small-disturbance (or small-signal) rotor angle stability

Small-disturbance rotor angle stability is concerned with the ability of the power system to maintain synchronism under small disturbances. The disturbances are considered to be sufficiently small that linearization of system equations is permissible for purposes of analysis [20].

Small-disturbance stability depends on the initial operating state of the system. Instability that may result can be of two forms [20]:

I) Increase in rotor angle through a non-oscillatory or aperiodic mode due to lack of synchronizing torque [20], or

II) Rotor oscillations of increasing amplitude due to lack of sufficient damping torque [20].

The nature of system response to small disturbances depends on a number of factors including the initial operating, the transmission system strength, and the type of generator excitation controls used. For a generator connected radially to a large power system, in the absence of automatic voltage regulators (i.e. with constant field voltage) the instability is due to lack of sufficient synchronizing torque. This results in instability through a non-oscillatory mode, as shown in Figure 2.2(a). With continuously acting voltage regulators, the small-disturbance stability problem is one of ensuring sufficient damping of system oscillations. Instability is normally through oscillations of increasing amplitude. Figure 2.2(b) illustrates the nature of generator response with automatic voltage regulators [1].

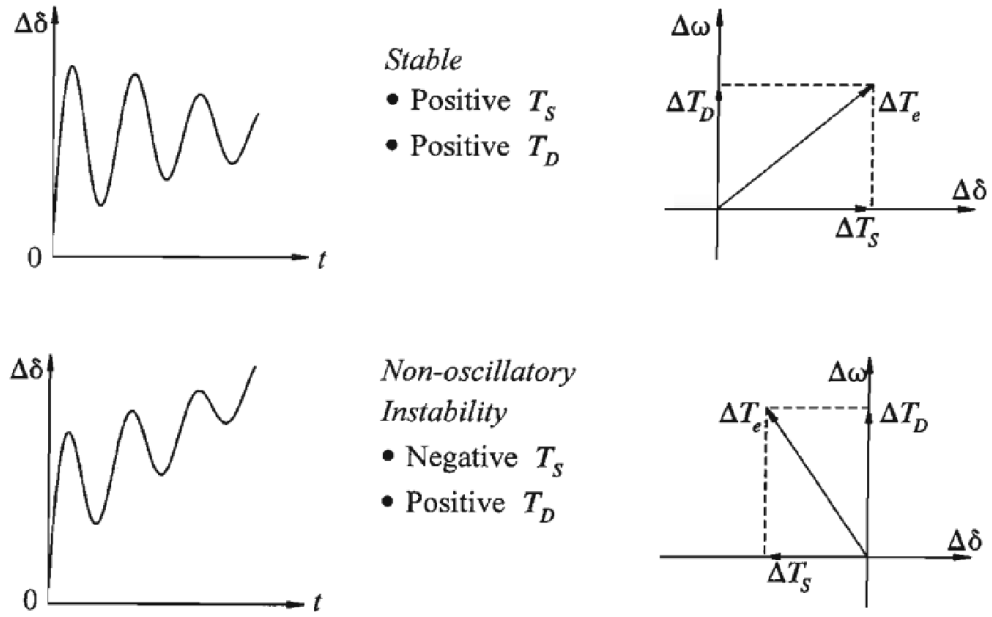

(a) With constant field voltage

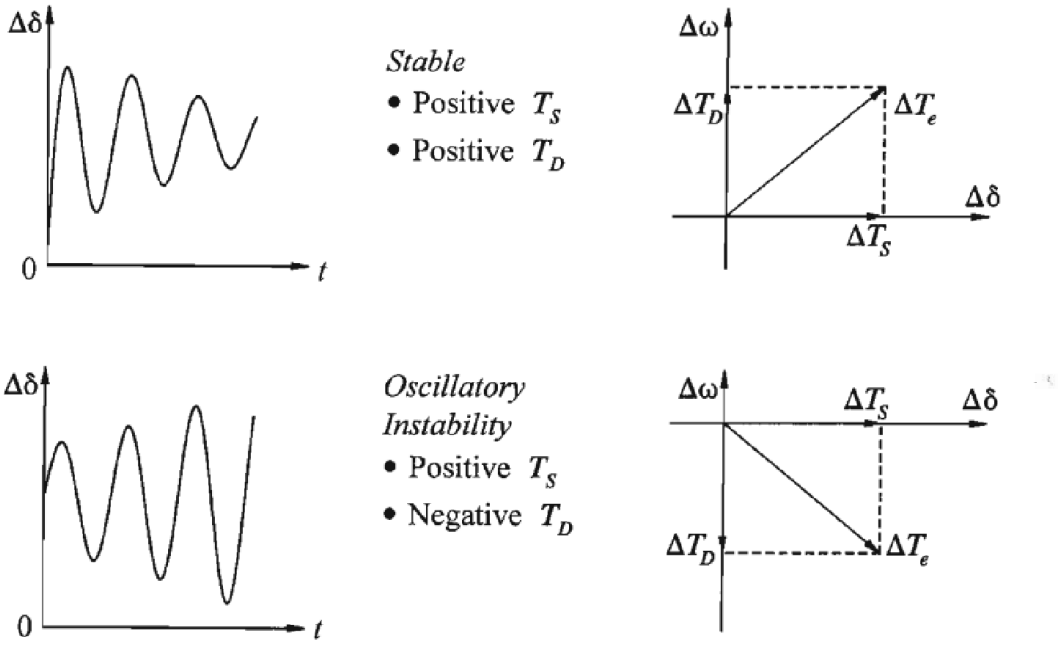

(b) With excitation control

Fig.2.2 Nature of small-disturbance response

In today's practical power system, small-signal stability is largely a problem of insufficient damping of oscillations. The stability of the following types of oscillations is concern:

a) Local Plant Mode Oscillations

Local problems involve a small part of the power system, and are usually associated with rotor angle oscillations of a single power plant against the rest of the power system. Such oscillations are called local plant mode oscillations [20].

Stability (damping) of these oscillations depends on the strength of the transmission system as seen by the power plant, generator excitation control systems and plant output [20]. The frequency of local modes is usually in the range of 1 to 2 HZ.

b) Inter-Area Mode Oscillations

Global problems are caused by interactions among large groups of generators and have widespread effects. They involve oscillations of a group of generators in one area swinging against a group of generators in another area. Such oscillations are called inter-area mode oscillations. Their characteristics are very complex and significantly differ from those of local plant mode oscillations. Load characteristics, in particular, have a major effect on the stability of inter-area modes [20]. The frequency range of inter-area modes is within 0.2 and 1 HZ.

c) Control Modes

Control modes are associated with generating units and other controls. Poorly tuned exciter, speed governors, HVDC converters and static var compensators are the usual

causes of instability of these modes [1]. The frequency range of these modes is greater than 4 HZ.

d) Torsional Modes

Torsional modes are associated with the turbine-generator shaft system rotational components. Instability of torsional modes may be caused by interaction with excitation controls, speed governors, HVDC controls, and series-capacitor-compensated lines [1]. The frequency of torsional modes is greater than 4 HZ.

The time frame of interest in small-disturbance stability studies is on the order of 10 to 20 seconds following a disturbance [20].

2.3.4 Comments on Classification

Power system stability has been classified for convenience in identifying causes of instability, applying suitable analysis tools, and developing corrective measures. In any given situation, however, any one form of instability may not occur in its pure form. This is particularly true in highly stressed systems and for cascading events; as systems fail one form of instability may ultimately lead to another form. However, distinguishing between different forms is important for understanding the underlying causes of the problem in order to develop appropriate design and operating procedures [18].

While classification of power system stability is an effective and convenient means to deal with the complexities of the problem, the overall stability of the system should always be kept in mind. Solutions to stability problems of one category should not be at

the expense of another. It is essential to look at all aspects of the stability phenomenon and at each aspect from more than one viewpoint [18].

2.4 Modal analysis

Modern power system is a large-scale, non-linear and dynamic system. Its stability analysis is one of the most important problems in power system operation and control research area [21].

The stability of the non-linear system can usually be judged by the eigenvalues of its linearized system [21].

2.4.1 state space representation

A power system may be described by a set of (n) first order nonlinear ordinary differential equation of the following form [1]:

$$\dot{x}_i = f1(x_1, x_2, \ldots, x_n ; u_1, u_2 , \ldots, u_r ; t) \qquad i = 1,2,\ldots, n \qquad (2.2)$$

Where (n) is the order of the system and (r) the number of input. This can be written in the vector-matrix notation:

$$\dot{x} = f(x, U, t) \qquad (2.3)$$

Where

$$x=\begin{bmatrix} x1 \\ x2 \\ : \\ xn \end{bmatrix} \qquad u=\begin{bmatrix} u1 \\ u2 \\ : \\ ur \end{bmatrix} \qquad f=\begin{bmatrix} f1 \\ f2 \\ : \\ fn \end{bmatrix}$$

The column vector (x) is referred as the state vector, and its entries (xi) as state variables, the column vector (u) is the vector of inputs to the system. These are the external signals that influence the performance of the system. Time is denoted by (t), the derivative of the state variable (x) with respect to time is denoted by $\dot{x}$, if the derivative of the state variables is not explicit function of time, eqn. (2.2) simplified to

$$\dot{x} = f(x, u) \qquad (2.4)$$

The output variables in terms of the state variables and the input variables can be written in the following form

$$Y = g(x, u) \qquad (2.5)$$

Where

$$Y = \begin{bmatrix} y1 \\ y2 \\ : \\ ym \end{bmatrix} \qquad g = \begin{bmatrix} g1 \\ g2 \\ : \\ gn \end{bmatrix}$$

2.4.2 Linearization

Small-signal stability defined in the context of a power system is the ability to maintain synchronism when subjected to small perturbations [1]. The term 'small' implies that the equations describing the response may be linearized for analysis, which is the focus of this section [22].

Let (x_0) be the initial state vector and our input vector corresponding to the equilibrium point about which the small signal performance is to be investigated. Since (x_0) and (u_0) satisfy eqn. (2.3), we have

$$\dot{x}_0 = f(x_0, u_0) = 0 \qquad (2.6)$$

Let us perturb the system from the above state, by letting

$$x = x_0 + \Delta x \qquad u = u_0 + \Delta u$$

The new state must satisfy eqn. (2.3), hence

$$\dot{x} = \dot{x}_0 + \Delta\dot{x} = f[(x_0 + \Delta x), (u_0 + \Delta u)] \qquad (2.7)$$

As the perturbation is assumed to be small, the nonlinear function f (x,u) can be expressed in terms of Taylor's series expansion. With terms involving second and higher order powers of Δx and Δu neglected, we may write

$$\dot{x}_i = \dot{x}_{i0} + \Delta\dot{x}_{io} = f_i[(x_0 + \Delta x), (u_0 + \Delta u)]$$

$$= f_i(x_0, u_0) + \frac{\partial fi}{\partial x1}\Delta x_i + \ldots + \frac{\partial fi}{\partial xn}\Delta x_n$$

$$+ \frac{\partial fi}{\partial u1}\Delta u_i + \ldots + \frac{\partial fi}{\partial ur}\Delta u_n$$

Since $\dot{x}_{i0} = f_i(x_0, u_0)$, we obtain

$$\Delta\dot{x}_i = \frac{\partial fi}{\partial x1}\Delta x_i + \ldots + \frac{\partial fi}{\partial xn}\Delta x_n + \frac{\partial fi}{\partial u1}\Delta u_i + \ldots + \frac{\partial fi}{\partial ur}\Delta u_n$$

With i = 1, 2,…, n. In a like manner, from eqn. (2.4) we have

$$\Delta y_j = \frac{\partial gi}{\partial x1}\Delta x_i + \ldots + \frac{\partial gi}{\partial xn}\Delta x_n + \frac{\partial gi}{\partial u1}\Delta u_i + \ldots + \frac{\partial gi}{\partial ur}\Delta u_n$$

With j = 1, 2,… , m. Therefore the linearized form of eqn. (2.3) and (2.4) are shown in fig. (2.3)

$$\Delta\dot{x} = A\,\Delta x + B\,\Delta u \qquad (2.8)$$

$$\Delta y = C\,\Delta x + D\,\Delta u \qquad (2.9)$$

Where

$$A = \begin{bmatrix} \frac{\partial f1}{\partial x1} & \cdots & \frac{\partial f1}{\partial xn} \\ \cdots & \cdots & \cdots \\ \frac{\partial fn}{\partial x1} & \cdots & \frac{\partial fn}{\partial xn} \end{bmatrix} \qquad B = \begin{bmatrix} \frac{\partial f1}{\partial u1} & \cdots & \frac{\partial f1}{\partial ur} \\ \cdots & \cdots & \cdots \\ \frac{\partial fn}{\partial u1} & \cdots & \frac{\partial fn}{\partial ur} \end{bmatrix}$$

$$C = \begin{bmatrix} \frac{\partial g1}{\partial x1} & \cdots & \frac{\partial g1}{\partial xn} \\ \cdots & \cdots & \cdots \\ \frac{\partial gm}{\partial x1} & \cdots & \frac{\partial gm}{\partial xn} \end{bmatrix} \qquad D = \begin{bmatrix} \frac{\partial g1}{\partial u1} & \cdots & \frac{\partial g1}{\partial ur} \\ \cdots & \cdots & \cdots \\ \frac{\partial gm}{\partial u1} & \cdots & \frac{\partial gm}{\partial ur} \end{bmatrix}$$

The above partial derivatives are evaluated at the equilibrium point about which the small perturbation is being analyzed.

In equations (2.7) and (2.8);

Δx: is the state vector of dimension n.

Δy: is the output vector of dimension m.

Δu: is the input vector of dimension r.

A: is the state or plant matrix of size n×n.

B: is the control or input matrix of size n×r.

C: is the output matrix of size m×n.

D: is the (feed forward) matrix which defines the proportion of input which appears directly in the output, size m×r.

By taking the Laplace transform of the above equations, we obtain the state space equation in the frequency domain as:

$$S\,\Delta x(s) - \Delta x(0) = A\,\Delta x(s) + B\,\Delta u(s) \qquad (2.10)$$

$$\Delta y(s) = C\,\Delta x(s) + D\,\Delta u(s) \qquad (2.11)$$

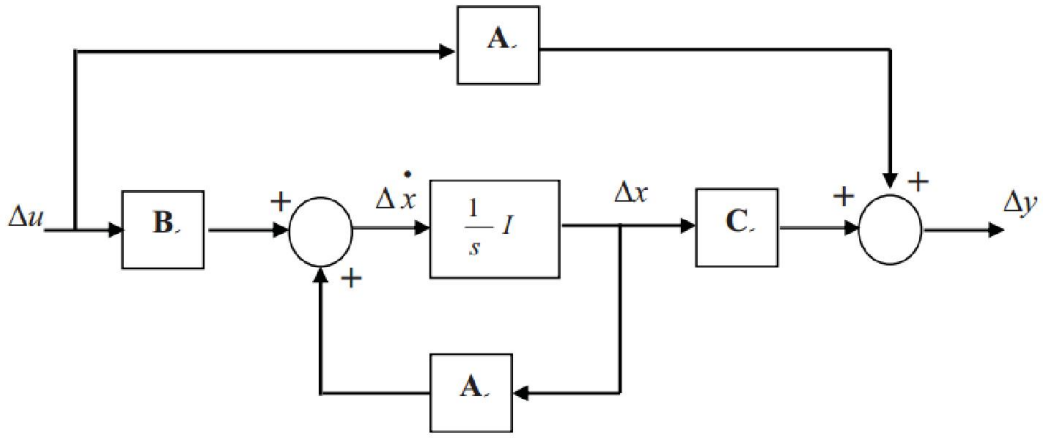

Fig.2.3 Block diagram of the state space representation

2.4.3 Eigenvalues and Stability

The stability of the non-linear system can usually be judged by the eigenvalues of its linearized system [21]. Therefore, the stability of the system is determined by the eigenvalues as follow [1]:

A real eigenvalue corresponds to a non-oscillatory mode. A negative real eigenvalue represents a decaying mode. The larger its magnitude, the faster the decay. A positive real eigenvalue represents non oscillating mode instability [1].

Complex eigenvalue occur in conjugate pairs, And each pair corresponds to an oscillatory mode. The real component of the eigenvalues gives the damping, and the

imaginary component gives the frequency of oscillation. A negative real part represents a damped oscillation where as a positive real part represents oscillation of increasing amplitude, thus for a complex pair of Eigenvalues:

$$ƛ = \sigma \pm j\,\omega \qquad (2.12)$$

The frequency of oscillation in Hz is given by:

$$F = \frac{\omega}{2\pi} \quad (Hz) \qquad (2.13)$$

And the damping ratio is given by:

$$\zeta = \frac{-\sigma}{\sqrt{\sigma^2+\omega^2}} \qquad (2.14)$$

The damping ratio ζ determines the rate of decay of the amplitude of the oscillation. The time constant of amplitude decay is 1/|σ|. In other words, the amplitude decays to 1/e or 37% of the initial amplitude in 1/|σ| seconds or in 1/(2 π ζ) cycles of oscillation [1].

Fig.2.4 shows the six different eigenvalue combinations and the corresponding trajectory behavior.

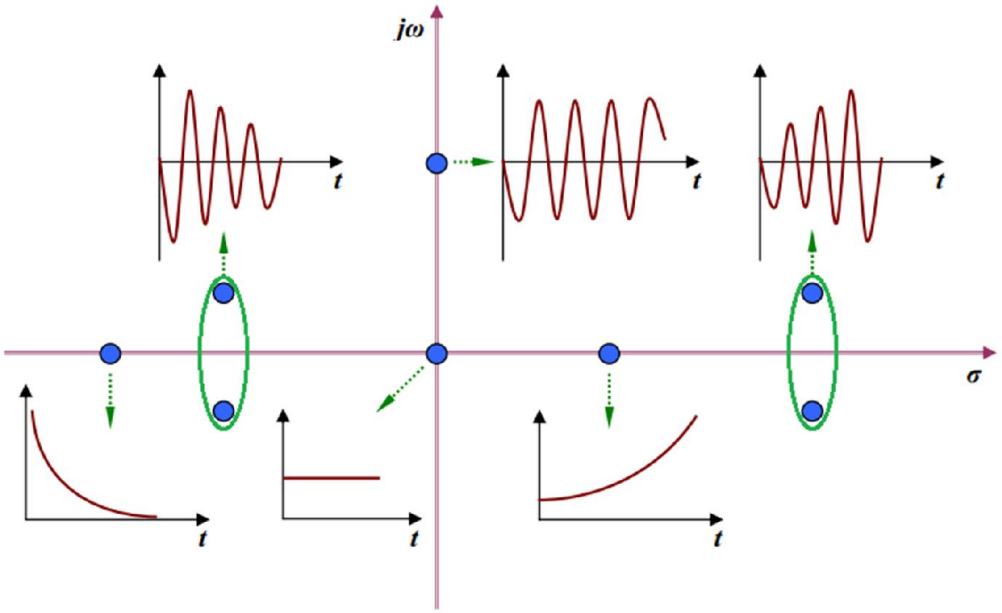

Fig.2.4 Eigen values effect on system stability

There is no one-to-one relationship between any single eigenvalue and a particular state because they each belong to the system as a whole. It is therefore necessary to define the participation matrix P which provides a numerical score of a particular eigenvalue against a specific state. The participation matrix is generated from the matrices of right and left eigenvalues, Φ and Ψ respectively. Note that it is standard practice to normalize these matrices such that ΨΦ=I [22].

$$\Phi=[\phi 1 \phi 2 \ldots \phi n] \qquad (2.15)$$

$$\Psi=[\psi T1 \psi T2 \ldots \psi Tn]T \qquad (2.16)$$

Where the right and left eigenvectors are given by Equations (2.16) and (2.17) respectively

$$A\phi i=\lambda\phi i=0 \qquad (2.17)$$

$$\psi iA=\lambda\psi i=0 \qquad (2.18)$$

$$\phi i = \begin{bmatrix} \phi 1i \\ \phi 2i \\ ... \\ \phi ni \end{bmatrix} \quad ; \quad \psi i=[\psi 1i \psi 2i \ldots \psi ni] \qquad (2.19)$$

The modal matrices Φ and Ψ are then used to form the participation matrix P, the entries of which will be used to determine the dominant eigenvalues for each state.

$$P=[p_1\ p_2\ \ldots\ p_n] \qquad (2.20)$$

Where $$pi = \begin{bmatrix} \phi 1i\psi i1 \\ \phi 2i\psi i2 \\ ... \\ \phi ni\psi in \end{bmatrix}$$

ϕki= kth row, ith column of modal matrix Φ.

ψik=ith row, kth column of modal matrix Ψ.

2.5 Conclusion

The concept and categorization of power system stability is introduced in this chapter. Furthermore, the variables influencing system stability are discussed, followed by a comprehensive modal analysis for analyzing small signal stability.

Chapter III

Power System Stabilizer Optimization

Using PSO Algorithm

Chapter III: Power System Stabilizer Optimization Using PSO Algorithm

3.1 Introduction

Iterative optimization is as old as life itself. Even very primitive beings act according to a simple impulse that can be summarized in a few words: “To improve their situation”. It is therefore not surprising that, explicitly or implicitly, several mathematical models of optimization take as a starting point biological behaviors and make an abundant use of metaphors and terms originating from genetics, ethology, and even from ethnology or psychology [23].

Optimization techniques proved to be effective tools to resolve many power system problems and those they could be more effective when properly joined together with conventional mathematical approaches [24].

Swarm intelligence is one of the optimization techniques that is used to solve modern power system optimization problems. Swarm Intelligence (SI) is a term referring to the collective behavior of limited capabilities set of similar objects. Although the individual behavior is far from achieving a goal by itself, the collective behavior archives such a goal. Examples of systems like this can be found in nature, including ant colonies, bird flocking, animal herding, bacteria molding and fish schooling [25]. The advantage of these approaches over traditional techniques is their robustness and flexibility. These properties make swarm intelligence a successful design paradigm for algorithms that deal with increasingly complex problems [25]. One successful examples of optimization techniques inspired by swarm intelligence is: particle swarm optimization (PSO).

3.2 Particle Swarm Optimization

Particle swarm optimization (PSO) algorithm is a stochastic optimization technique based on swarm, which was proposed by Kennedy and Eberhart (1995) [26]. PSO is a global optimization algorithm for dealing with problems in which a best solution can be represented as a point or surface in an n-dimensional space. PSO simulates the behaviors of bird flocking. In PSO, each single solution is a "bird" in the search space that is called "particle". All of particles have fitness values which are evaluated by the fitness function to be optimized, and have velocities which direct the flying of the particles. The particles fly through the problem space by following the current optimum particles. PSO is initialized with a group of random particles (solutions) and then searches for optima by updating generations [25]. Each particle has a position and a velocity and has the memory ability, they can memorize the best position it ever reached, denoted as Pbest. The swarm can communicate in some way, and each individual is able to know and memorize the best location of the total swarm so far, marked as Gbest [26].

During the iteration, the update of the velocity of the ith particle is determined by Equation (3.1). The new position is then determined by the sum of the previous position and the new velocity by Equation (3.2).

$$v_i^{t+1} = w\, v_i^t + c_1 r_1 (P_i^t - X_i^t) + c_2 r_2 (G^t - X_i^t) \qquad (3.1)$$

$$X_i^{t+1} = X_i^t + v_i^{t+1} \qquad (3.2)$$

Where:

v_i^{t+1}: Velocity of particle i at *t+1* th iteration.

v_i^t: Velocity of particle i at *t* th iteration.

X_i^{t+1}: Position of particle i at *t+1* th iteration.

X_i^t: Position of particle i at *t* th iteration.

c_1, c_2: positive numbers illustrating the weights of the acceleration terms that guide each particle toward the individual best and the swarm best positions respectively.

w: inertial weight which controls the exploitation of the search space.

r_1, r_2: random numbers between 0 and 1.

G: Gbest position of swarm.

P: Pbest position of particle.

Updating process of velocity and position of each particle is depicted in Fig. 3.1.

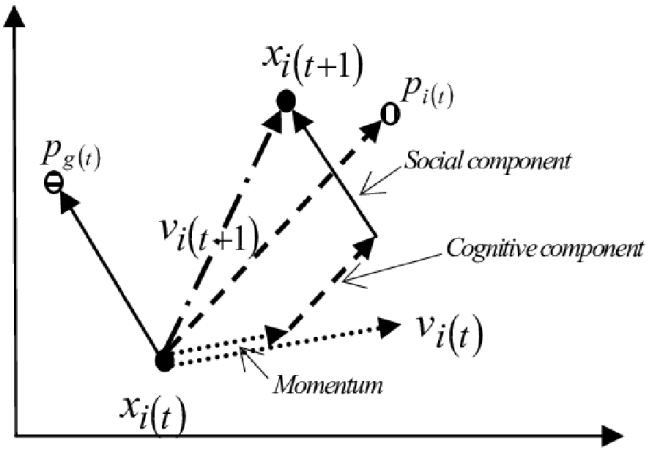

Fig. 3.1 The velocity and position updates in PSO.

Chapter III: Power System Stabilizer Optimization Using PSO Algorithm

An algorithm to find the best positioning vector of PSO using n particles can be summarized as follows:

1. At the first step, initialize n particles with random positions and random velocities for d-dimensions.
2. Evaluate the fitness of each particle in the swarm, take the positions of the particles into a target function J, and get the result of the function.
3. For each iteration, compare the value of each particle with its Pbest. If the current value is better than Pbest, set Pbest to be equal to the current value and the position of Pbest to be the current location in the d-dimensional space. Compare Pbest with Gbest. If Pbest is better than Gbest, set the position of Gbest to be that of Pbest and Gbest to be equal to Pbest in the d-dimensional space.
4. Compare Gbest with the target. If the result is satisfactory, the position of Gbest is the solution that is desired. If not, let the particles move to new positions to find fine answers.
5. The velocity and position of the *i* th particle are changed according to equations (3.1) and (3.2).
6. Vmax/Vmin is the maximum/minimum allowable velocity for the particles. If the velocity of the particle v_i^{t+1} is not in [Vmin, Vmax], the velocity will be limited to Vmin/Vmax. The particle position is also limited in a certain range. If X_i^{t+1} is out of the range, it will be pulled back to the edge.
7. Repeat Steps (2) to (6) until the request of Step (4) fits or the max step is reached.

Fig. 3.2 shows a general flowchart of the particle swarm optimization algorithm.

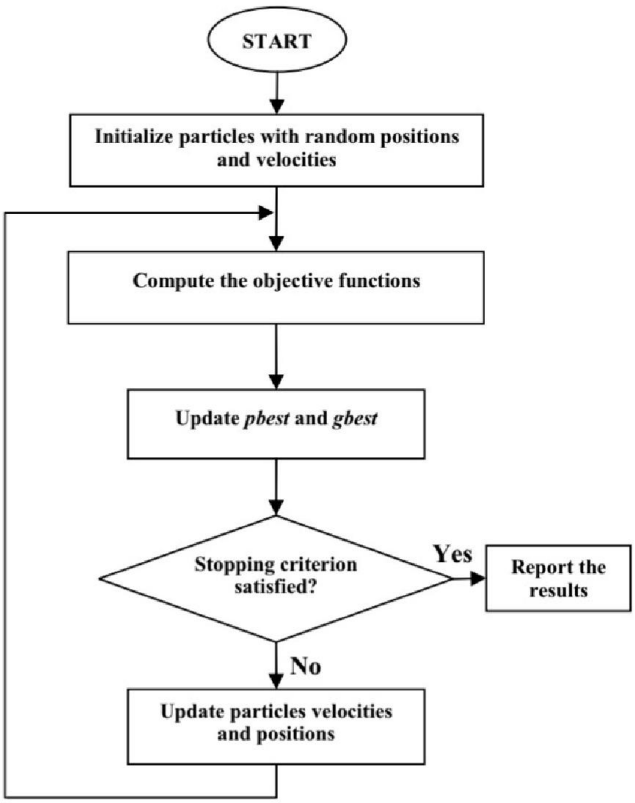

Fig. 3.2 PSO algorithm flowchart

3.3 Why PSO?

PSO algorithm is one of the optimization techniques used to solve PSS tuning problem. There are many techniques used for the same purpose. Some of these techniques are: Artificial Neural Network (ANN), Fuzzy Logic Control (FLC), and other optimization algorithms such as: BAT algorithm, Genetic algorithm, and Tabu search. Choosing PSO is not a random choice, it has some advantages over the other techniques:

* It has been found to be robust in solving problems featuring non-linearity, non-differentiability and high dimensionality [27].

* Unlike the other heuristic techniques, it has a flexible and well-balanced mechanism to enhance the global and local exploration abilities [27].

* It suffices to specify the objective function and to place finite bounds on the optimized parameters [27].

* Particle swarm optimization, does not require any gradient information of the function to be optimized, uses only primitive mathematical operators and is conceptually very simple [25].

3.4 Proposed approach

The aim of this project is the optimal tuning of the PSS parameters in a multi-machine power system using PSO algorithm. The PSO algorithm is written in a script Matlab code and the power system is represented by its Simulink model. Two objective functions are being used for optimizing the PSS parameters, one of which is time domain based and the other one is eigenvalues based. The data is exchanged between the script and the Simulink as follows:

* A particle from the swarm is exported from the script to the Simulink.

* The simulation is done and the output is either the rotor speed of the four generators or the eigenvalues of the system, which are stored in the workspace.

* The cost function is then calculated using the information from workspace.

* The personal and global bests values are updated according to the cost function.

* The velocity and the position of each particle are updated using the new values of Pbest and Gbest.

* Every particle must pass through the above-described sequence.

* This process is repeated until the stopping criterion is satisfied.

3.5 Objective Functions

The design problem is converted to an optimization problem. Therefore, an objective function (cost function) must be formulated to determine optimal parameters of multiple PSSs. Two objective functions are used for this study, the first is time domain based and is defined as follows:

$$J = \sum_{j=2}^{4} \int_{0}^{t_{sim}} t^2 \left(\Delta\omega_{1j}{}^2 + 0.34\,\Delta\omega_{3\ 4}^{\ 2}\right) dt \qquad (3.3)$$

The ranges of the optimized parameters are chosen to be as follows:

$$1 \leq k_i \leq 50$$

$$0.01 \leq T1_i \leq 2$$

$$0.01 \leq T2_i \leq 2$$

$$0.01 \leq T3_i \leq 2$$

$$0.01 \leq T4_i \leq 2$$

Where, t_{sim} is the time range of simulation, $\Delta\omega_{ij}$ is the relative rotor speed of the i th generator than the j th generator, k_i is the stabilizer gain, and $\{T1_i, T2_i, T3_i, T4_i\}$ are the time constants of the two lead-lag circuits of the PSS.

This objective function is used because it requires the minimal dynamic plant information. It is also used to guarantee stability by maintaining the four machines in synchronism.

The second objective function (eigenvalues based) is defined below:

$$J = J1 + \alpha J2 \qquad (\alpha = 10) \qquad (3.4)$$

$$J1 = \sum_{i=1}^{n} (\sigma_0 - \sigma_i)^2 \qquad for\ \sigma_i \geq \sigma_0 \quad (\sigma_0 = -1) \qquad (3.5)$$

$$J2 = \sum_{i=1}^{n} (\xi_0 - \xi_i)^2 \qquad for\ \xi_i \leq \xi_0 \quad (\xi_0 = 0.2) \qquad (3.6)$$

The range of the parameters is the same as the first objective function.

n denotes the total number of eigenvalues. Term J1 in the objective function controls the real part (σ) of eigenvalues and generally leads the eigenvalues of the system to the left side of imaginary axis in an area less than σ_0. The term J2 in the objective function brings the damping (ξ) of eigenvalues to the desired damping (ξ_0) and controls the overshoot of the system. Value of α obtained by experimentation and considered constant equal to 10 [29].

The stability of a power system can be determined based on its eigenvalues. Eigenvalues with large negative real parts ensure system stability. The overshoot and oscillations values are determined by the damping coefficient of the system, where any increase in the damping coefficient reduces oscillations and improves the stability of the system. [29].

3.6 Simulation results

At first, the two area four machine system is simulated with no PSS. Then the simulation is done including the classical PSS from Kundur book (reference [1]). At the end, the PSO algorithm is introduced to the system with two different objective functions and new PSS parameters will result. The eigenvalues are calculated and plotted in each case.

3.6.1 Case I: System without PSS

The eigenvalues of the system without PSS shown in Table 3.1 are plotted in Fig. 3.3

Mode N°	Eigenvalue	Damping Ratio	Frequency (Hz)
1	$\mathbf{0.2 \pm j6.1}$	-0.0327	0.97
2	$\mathbf{0.1 \pm j6.0}$	-0.0166	0.95
3	$\mathbf{0.4 \pm j3.9}$	-0.1020	0.62
4	$-0.2 \pm j0.5$	0.3713	0.08

Table 3.1 Eigenvalues of the system without PSS.

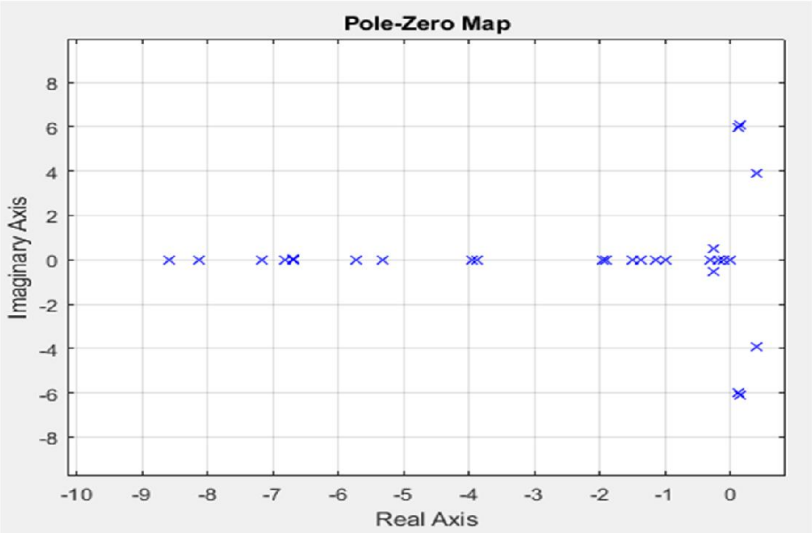

Fig. 3.3 Plot of eigenvalues of the system without PSS

It can be clearly seen from Table 3.1 and Fig. 3.3 that the system is unstable, since the eigenvalues are located in the real part of the plane (negative damping ratios).

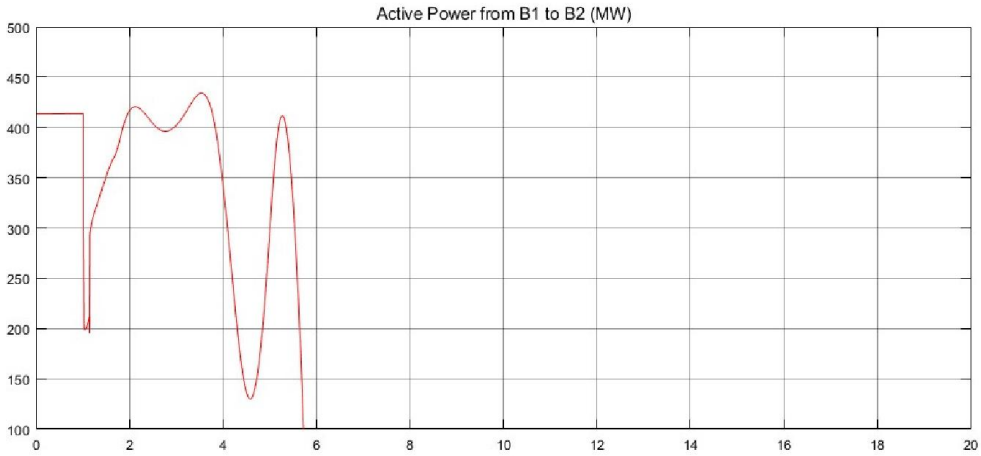

Fig. 3.4 Graph of active power from Area 1 to Area 2 of case 1

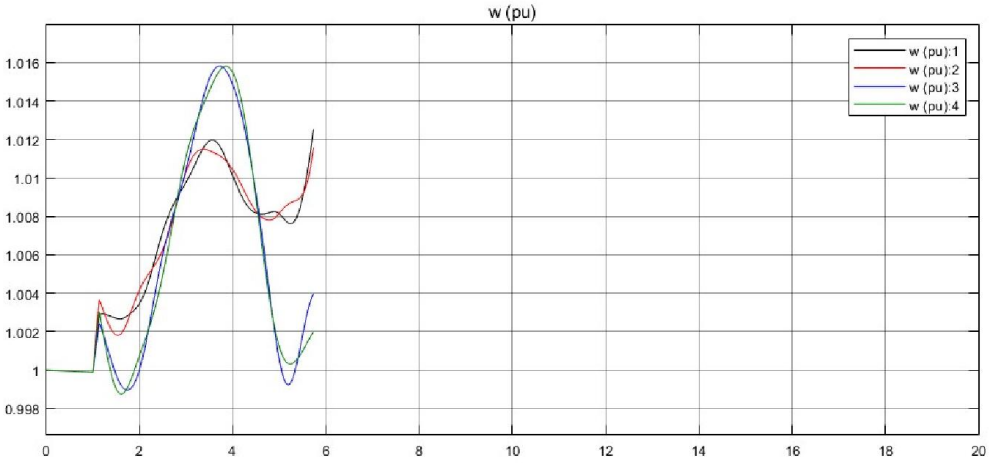

Fig. 3.5 Graph of the rotor speed of the four machines in pu of case 1

In the above figures, the simulation is not completed until the end because of the condition met in the system, stop simulation if the synchronism is lost. This shows how important is the PSS in the stability of power systems.

3.6.2 Case II: System with Kundur PSS

For this case a classical PSS is integrated to the system. The PSS parameters are tabled below:

Generator	Ks	T1	T2	T3	T4
1	30	0.05	0.02	3.0	5.4
2	30	0.05	0.02	3.0	5.4
3	30	0.05	0.02	3.0	5.4
4	30	0.05	0.02	3.0	5.4

Table 3.2 PSS parameters for the two-area four-machine system case 2.

The simulation of the system including the classical PSS gives the results below:

Mode N°	Eigenvalue	Damping Ratio	Frequency (Hz)
1	$-0.8 \pm j7.4$	0.1075	1.17
2	$-0.8 \pm j7.6$	0.1047	0.95
3	$-0.7 \pm j4.1$	0.1683	0.65
4	$-1.8 \pm j1.0$	0.8741	0.16

Table 3.3 Eigenvalues of the system with Kundur PSS.

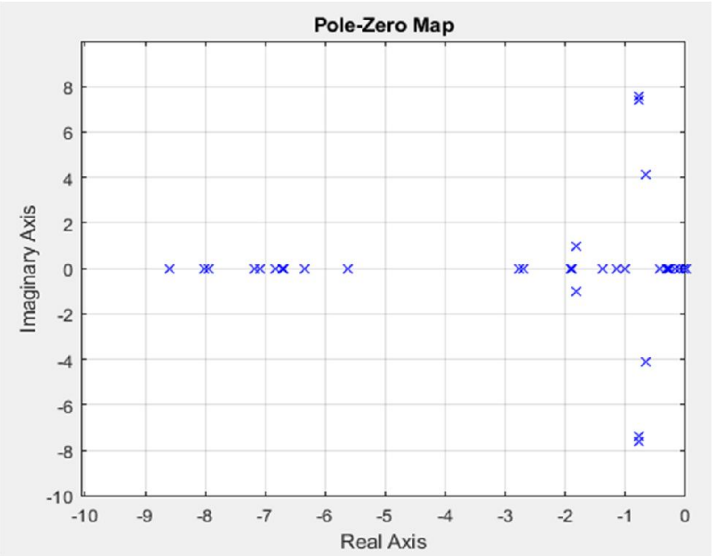

Fig. 3.6 Plot of eigenvalues of the system with Kundur PSS.

From the graph and the table of the eigenvalues, it can be seen that the eigenvalues have shifted to the left half plane which means that the stability of the system has enhanced. This yields the following graphs:

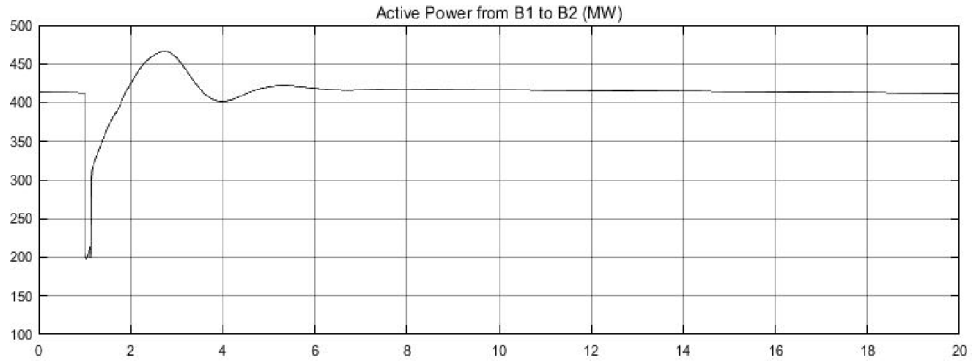

Fig. 3.7 Graph of active power from Area 1 to Area 2 of case 2.

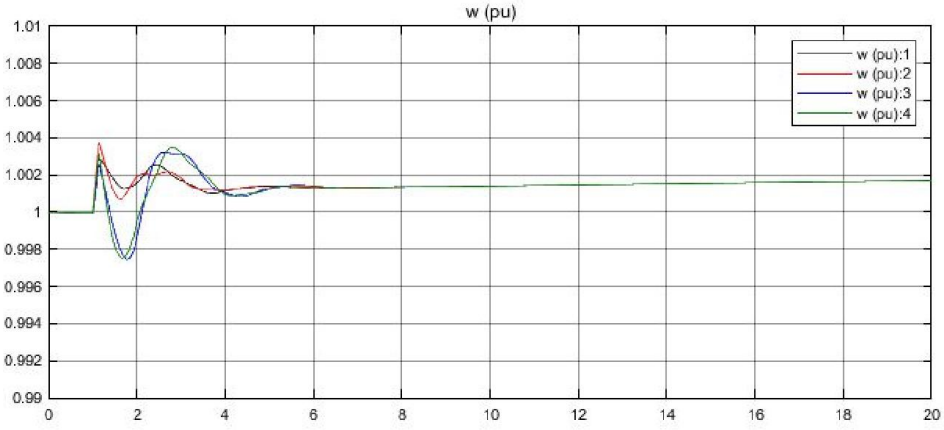

Fig. 3.8 Graph of the rotor speed of the four machines in pu of case 2.

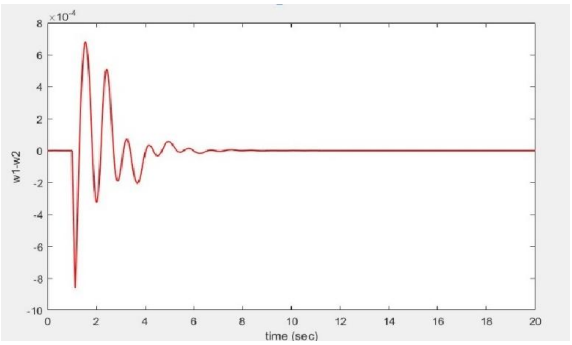

Fig. 3.9 Graph of w1-w2 case 2.

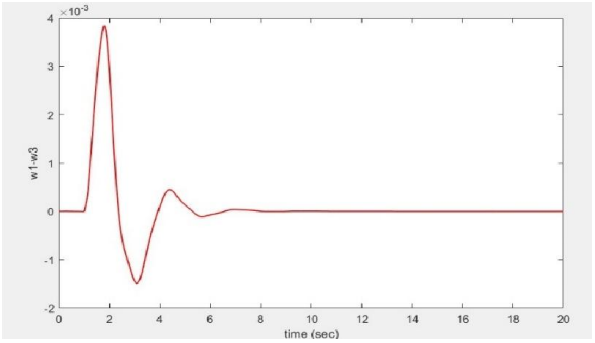

Fig. 3.10 Graph of w1-w3 case 2.

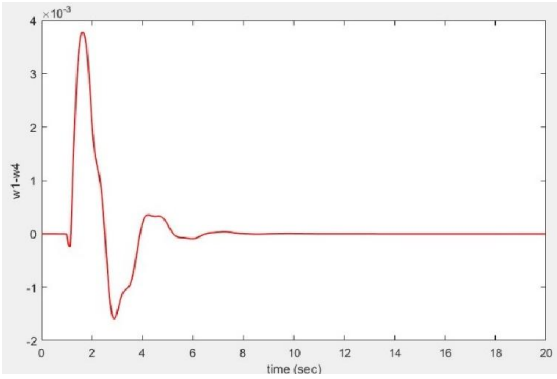

Fig. 3.11 Graph of w1-w4 case 2.

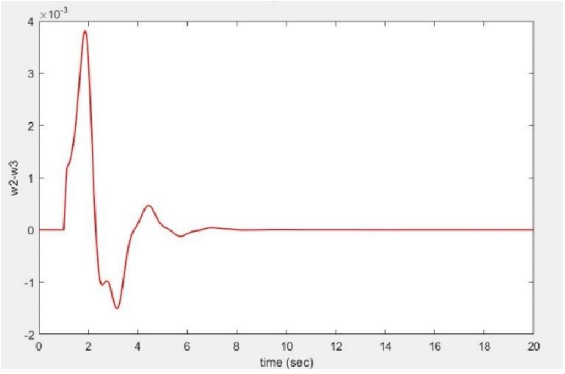

Fig. 3.12 Graph of w2-w3 case 2.

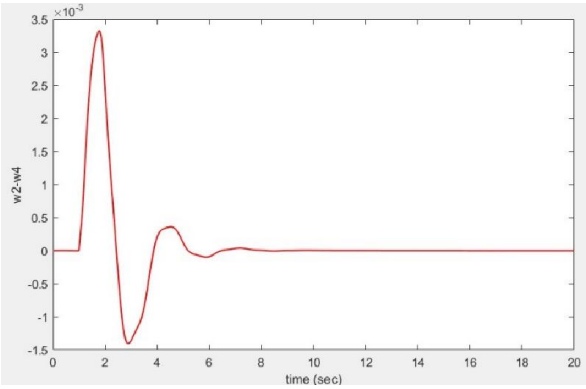

Fig. 3.13 Graph of w2-w4 case 2.

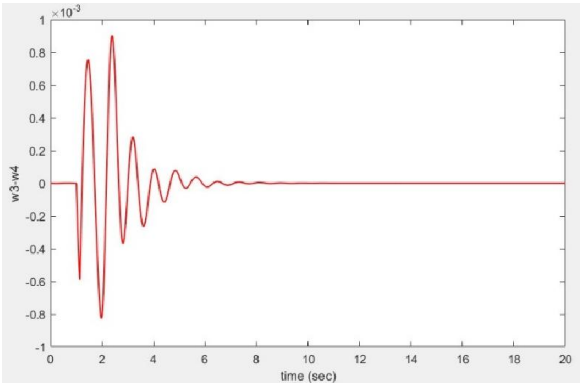

Fig. 3.14 Graph of w3-w4 case 2.

The above graphs show the difference between every two different rotor speeds of the four machines. Their settling time (the time to achieve steady state) and maximum overshoot are measured and tabled in Table 3.4.

Graph	Settling time	Maximum overshoot
w1-w2	8 sec	$7*10^{-4}$
w1-w3	7 sec	$3.8*10^{-3}$
w1-w4	6.5 sec	$3.8*10^{-3}$
w2-w3	7 sec	$3.8*10^{-3}$
w2-w4	7 sec	$3.4*10^{-3}$
w3-w4	8 sec	$0.9*10^{-3}$

Table 3.4 Settling time and Maximum overshoot of the graphs for case 2.

3.6.3 Case III: System with optimized PSS (PSOPSS)

a) First Objective function: The PSO algorithm is introduced to the system. The parameters of the PSO are chosen to be as follows:

Parameters	PSO
Swarm size	25
N° of iterations	100
C1	2
C2	2
Wmin	0.2
Wmax	0.9

Table 3.5 Parameters used for PSO algorithm case 3a.

The following results are those of the first objective function (Time-domain based). After 100 iterations, the fitness function or the change of objective function is illustrated in Fig. 3.15.

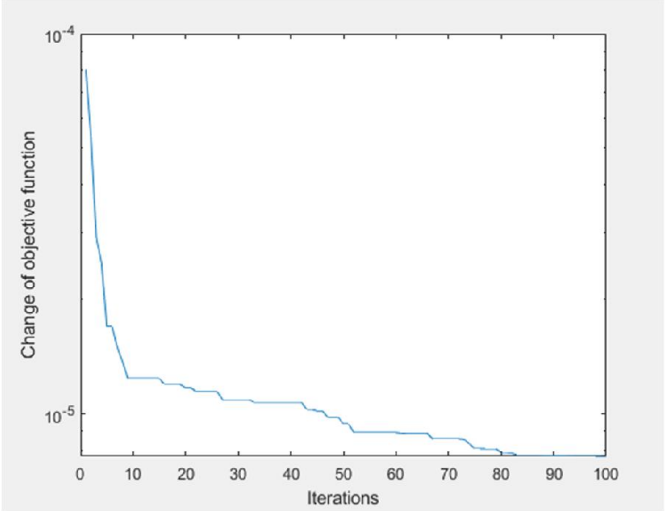

Fig. 3.15 Variations of objective function case 3a.

The obtained parameters for the four PSSs of the four machines are presented in Table 3.6.

	K	T1	T2	T3	T4
G1	50.0	1.22738	0.832078	0.695055	0.125747
G2	50.0	1.51627	0.0389789	1.20267	1.83618
G3	5.98097	1.04541	1.16095	1.6035	0.827891
G4	13.9812	0.451774	0.01	0.45983	0.569454

Table 3.6 Obtained Parameters of PSSs case 3a.

The eigenvalues of the resulted power system, after applying PSO, are shown in Table3.7 and plotted in Fig. 3.16.

Mode N°	Eigenvalue	Damping Ratio	Frequency (Hz)
1	$-2.5 \pm j19.7$	0.1260	3.14
2	$-1.2 \pm j6.0$	0.1961	0.95
3	$-0.8 \pm j2.7$	0.2841	0.43
4	$-0.8 \pm j1.1$	0.5882	0.18

Table 3.7 Eigenvalues of the system with optimized PSS (PSOPSS) case 3a.

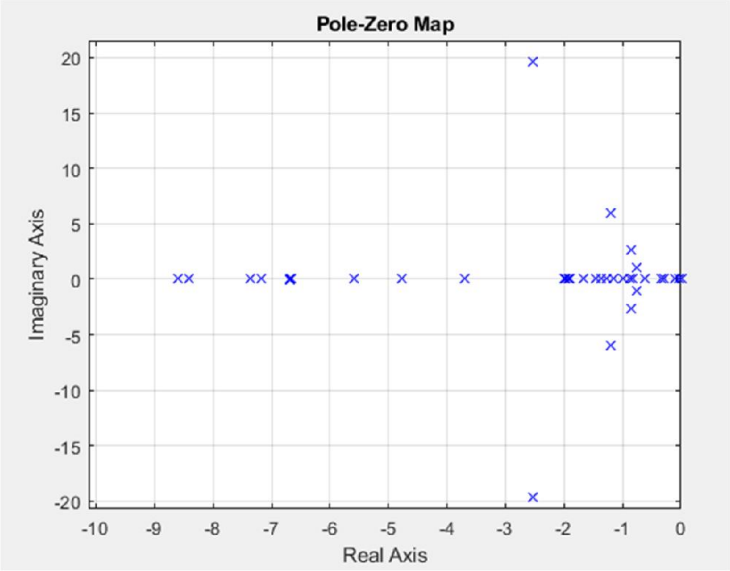

Fig. 3.16 Plot of eigenvalues of the system with optimized PSS (PSOPSS) case 3a.

Comparing the above results with the ones of Kundur PSS, it can be clearly seen that the damping ratios of the first three modes are increased and the placement of the eigenvalues in the S-plane are shifted more to the left. This means that the stability of the system has enhanced.

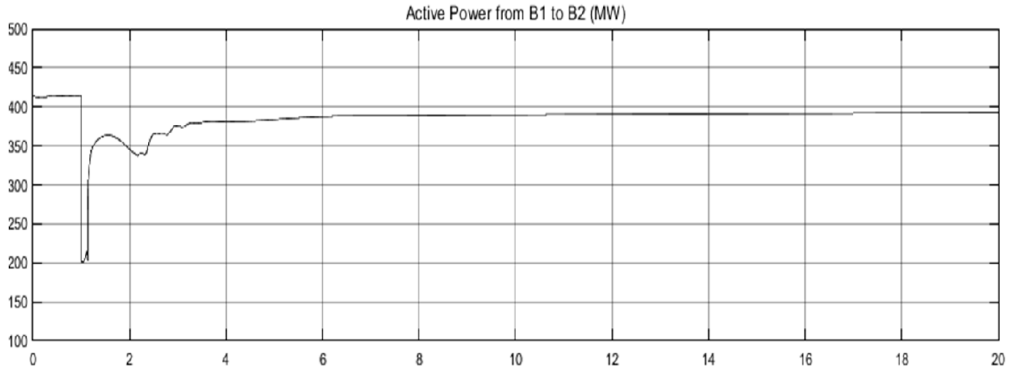

Fig. 3.17 Graph of active power from Area 1 to Area 2 of case 3a.

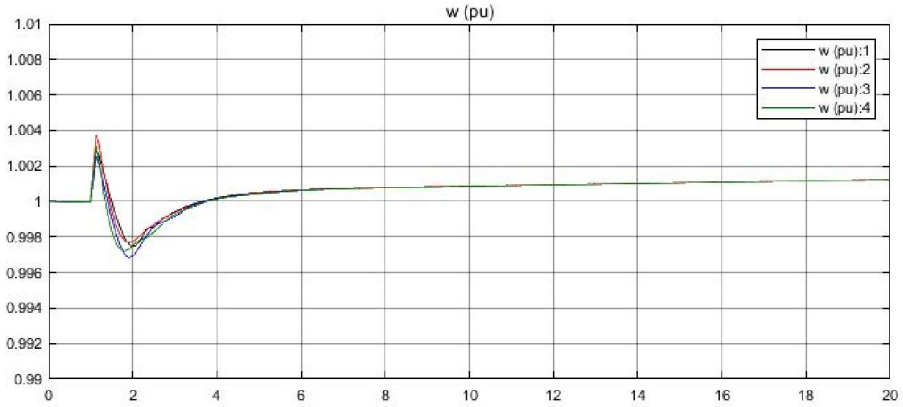

Fig. 3.18 Graph of the rotor speed of the four machines in pu of case 3a.

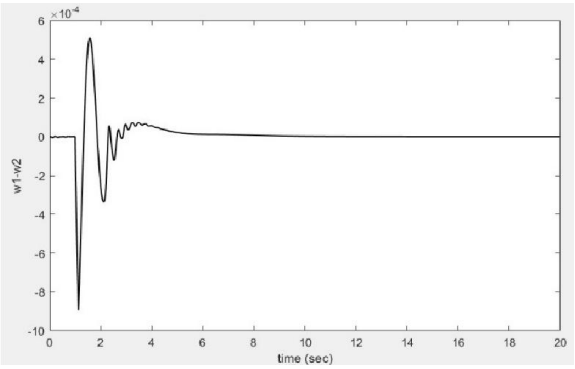

Fig. 3.19 Graph of w1-w2 case 3a.

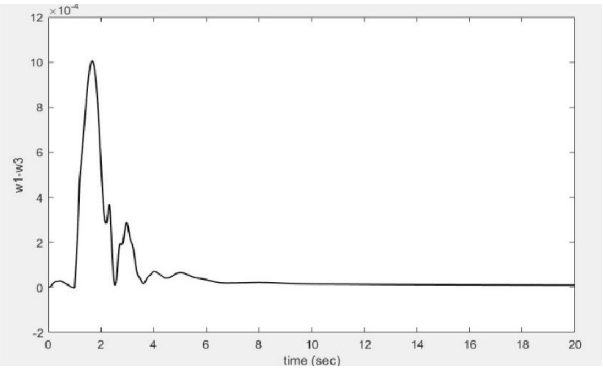

Fig. 3.20 Graph of w1-w3 case 3a.

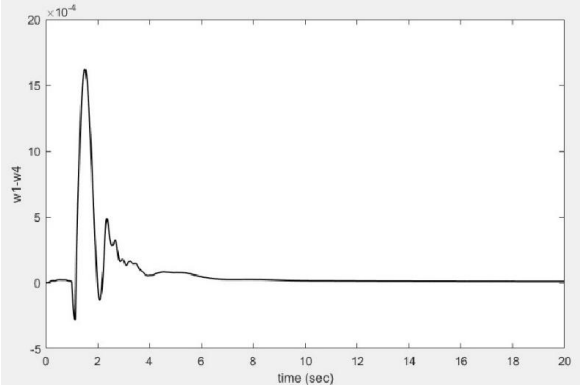

Fig. 3.21 Graph of w1-w4 case 3a.

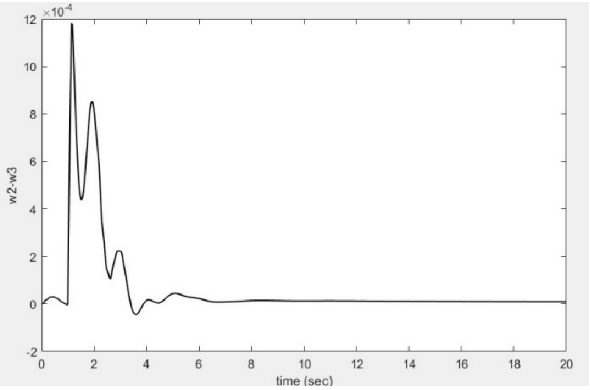

Fig. 3.22 Graph of w2-w3 case 3a.

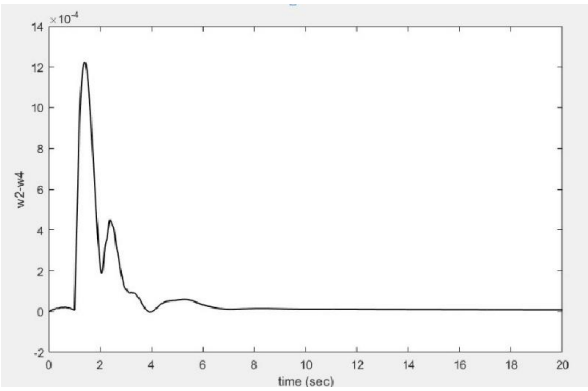

Fig. 3.23 Graph of w2-w4 case 3a.

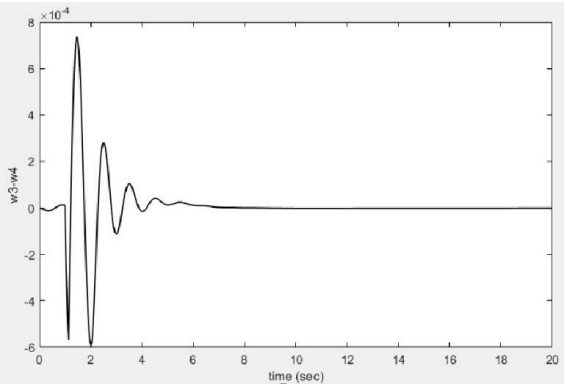

Fig. 3.24 Graph of w3-w4 case 3a.

Graph	Settling time	Maximum overshoot
w1-w2	5 sec	$5*10^{-4}$
w1-w3	6.1 sec	$1*10^{-3}$
w1-w4	6 sec	$1.6*10^{-3}$
w2-w3	6.2 sec	$1.2*10^{-3}$
w2-w4	6.3 sec	$1.2*10^{-3}$
w3-w4	6 sec	$0.72*10^{-3}$

Table 3.8 Settling time and Maximum overshoot of the graphs for case 3a.

Comparing the resultes in Table 3.8 with those of Table 3.4, it can be seen that the settling time and the maximum overshoots are getting smaller, which means that the synchronism of the system is improving.

b) Second Objective function: The parameters of the PSO for this case are chosen the same as case 3 except for the number of iterations which is changed to 300 iterations. The objective function for this case is plotted in following figure:

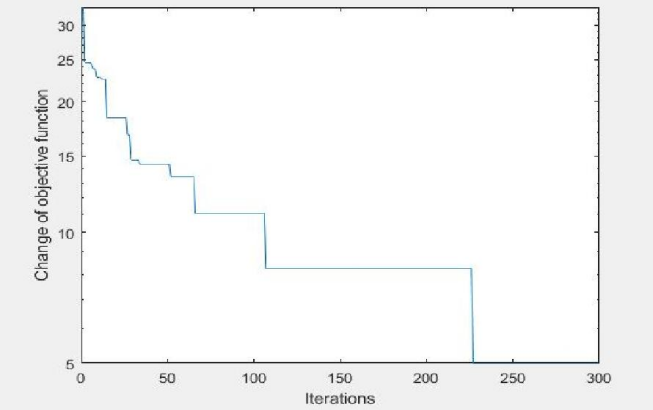

Fig. 3.25 Variations of objective function case 3b.

The obtained parameters for the four PSSs of the four machines are presented in Table 3.9.

	K	T1	T2	T3	T4
G1	20.3024	1.15503	0.182358	0.861029	1.22379
G2	23.5655	1.67057	1.06008	0.691276	1.71209
G3	42.0289	0.863335	1.26643	0.626951	0.788525
G4	33.4921	1.1536	1.14212	0.178752	0.0180081

Table 3.9 Obtained Parameters of PSSs case 3b.

Table 3.10 and Fig. 3.26 present the eigenvalues of the system for the 4th case.

Mode N°	Eigenvalue	Damping Ratio	Frequency (Hz)
1	$-1.7 \pm j8.1$	0.2054	1.28
2	$-1.5 \pm j2.3$	0.5463	0.36
3	$-1.7 \pm j1.9$	0.6668	0.30
4	$-1.7 \pm j0.5$	0.9594	0.08

Table 3.10 Eigenvalues of the system with optimized PSS (PSOPSS) case 3b.

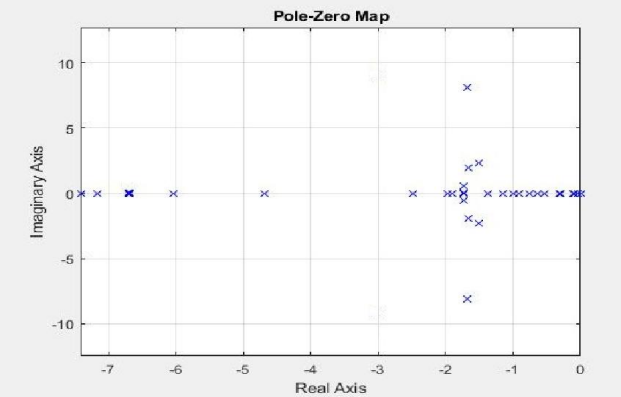

Fig. 3.26 Plot of eigenvalues of the system with optimized PSS (PSOPSS) case 3b.

From Fig. 3.26, it can be noticed that the eigenvalues of the system are more shifted to the left comparing to the results of the first objective function. This is because the second objective function is eigenvalues based.

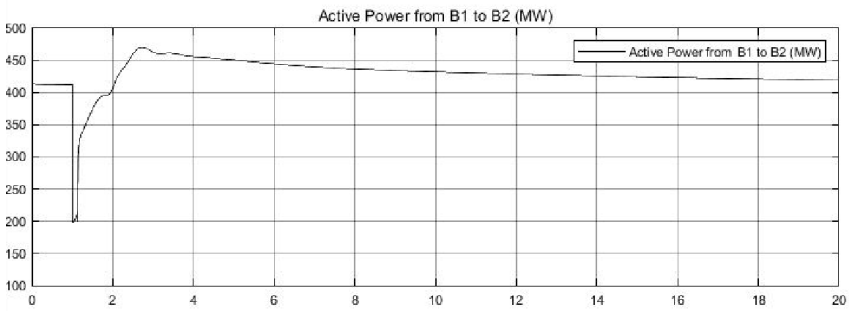

Fig. 3.27 Graph of active power from Area 1 to Area 2 of case 3b.

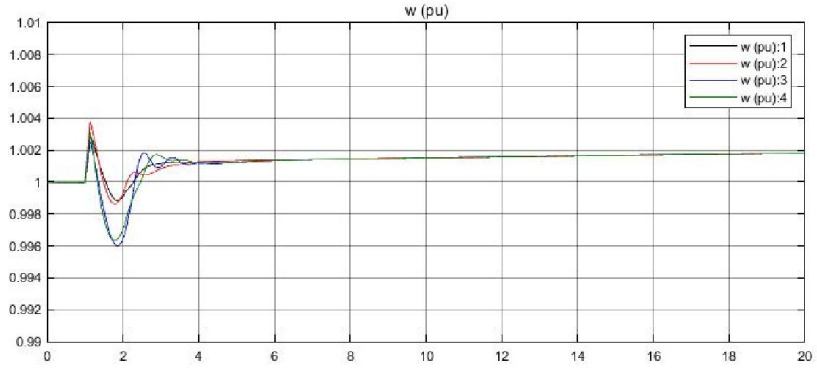

Fig. 3.28 Graph of the rotor speed of the four machines in pu of case 3b.

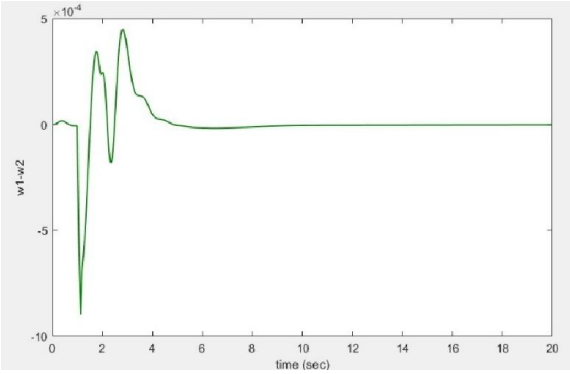

Fig. 3.29 Graph of w1-w2 case 3b.

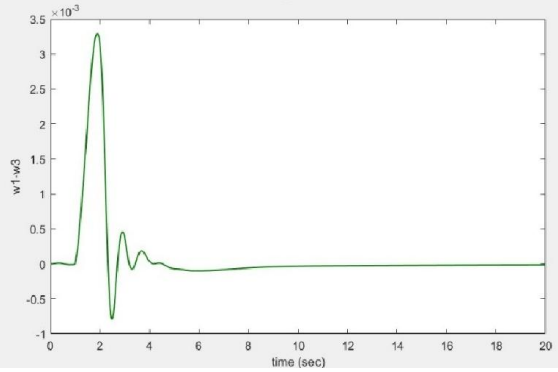

Fig. 3.30 Graph of w1-w3 case 3b.

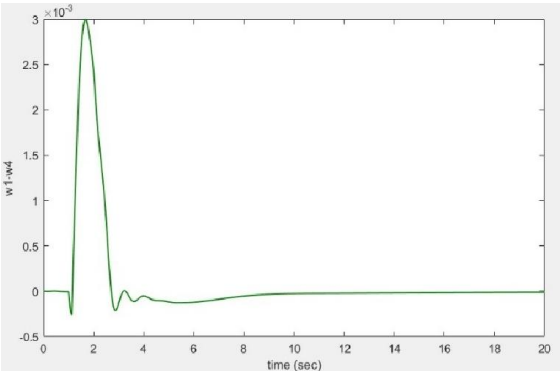

Fig. 3.31 Graph of w1-w4 case 3b.

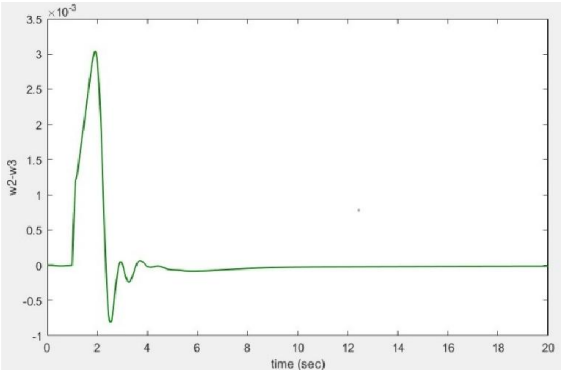

Fig. 3.32 Graph of w2-w3 case 3b.

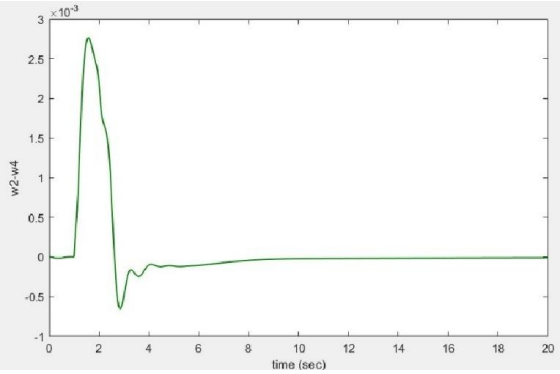

Fig. 3.33 Graph of w2-w4 case 3b.

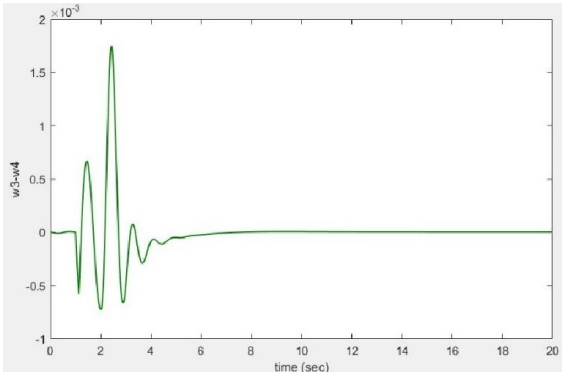

Fig. 3.34 Graph of w3-w4 case 3b.

Graph	Settling time	Maximum overshoot
w1-w2	4.6 sec	$4.4*10^{-4}$
w1-w3	5 sec	$3.25*10^{-3}$
w1-w4	4.3 sec	$3*10^{-3}$
w2-w3	4.5 sec	$3*10^{-3}$
w2-w4	4.5 sec	$2.75*10^{-3}$
w3-w4	5.1 sec	$1.75*10^{-3}$

Table 3.11 Settling time and Maximum overshoot of the graphs for case 3b.

3.7 Comments on the results

For the fisrt case, the system is simulated without including a PSS. The simulation results an unstable power system, some of its eigenvalues are located on the positive half of the S-plane. The output graphs are not finished till the end because the system becomes unstable.

In the second case, the system is supported with a classical PSS its data are taken from the Kundur refrence. The eigenvalues of the system are all plotted on the left part of the S-plane. Since the eigenvalues reflect the stability of the system, the system is considered to be stable. The settling time and the overshoot of the plotted graphs are recorded in Table 3.4, in order to compare them with other cases.

The third case is about optimization of the PSS parameters using PSO algorithm with the first objective function, which focuses on the rotor speed w of the four machines and trying to minimize the difference between them. As can be seen from Table 3.7 and Fig. 3.16 that the eigenvalues of the system are slightly better than those of case 2. While the measurment of the settling time and the overshoot of the graphs gives a better results compared with case 2.

The last case is also about the optimization of the parameters using PSO algorithm, but in this case a different objective function is being used. The main focus of this objective function is

the eigenvalues of the system. This would result that the eigenvalues are more shifted to the left than the other cases. This results in less speed overshoot and less settlint time.

3.8 Conclusion

In this chpater, three types of operations have been considered for the four generators power system that has been presneted in the previous chapter. Simulations with and without PSS while the parameters of this later have been quoted from Kundur [1]. The last operation of power system is considered while PSS paramters have been optimized using two different cost functions. The first one aims to minimize the difference in speeds while the second deals with the eignevalues of the concerned power system. As a result, the system is unsatble without PSS particularly when the system is operating near its limits. The computation of PSS parameters according to Kundur methodology allows to keep the system stable. Optimized PSS allows to improve better the stability (less oscillations and faster convergence) of the power system and this improvement depends on the selected cost function.

General Conclusion

The main objective of this work is the optimization of PSS parameters in a multimachine power system using PSO algorithm. The two-area four-machine power system is used for this study. The system is simulated in Simulink MATLAB and studied in three different cases:

*** Case I: System without PSS:**

The simulation in this case resulted an unstable system. The eigen analysis for this case gives positive eigenvalue and the resulted graphs show increasing oscillations. This shows how much the PSS is important to stabilize the system.

*** Case II: System with classical PSS:**

The classical PSS form reference [1] is added to the system. After simulation, the eigenvalues of the system show a stable system. The synchronization of the four machines is done after a while. The settling time and the maximum overshoot of the graphs of the difference in rotor speeds are measured in order to compare them with the rest of the results.

*** Case III: System with optimized PSS:**

PSO algorithm is introduced to the power system with two different objective functions. The first objective function is time domain based. After running the simulation with 100 iterations, new PSS parameters will result. The system is then simulated with these results. The output graphs show so much enhancement in the stability of the system, especially the synchronization of the four machines. This is proven by the measurement of the settling time and the maximum overshoot in Table 3.8.

The second objective is eigenvalues based. The PSS parameters that result after 300 iterations are put into the power system. The eigen analysis of the system show enhancement of the stability, especially in terms of the eigenvalues. The eigenvalues of the system have shifted more to the left than any case before.

As further work, we propose to extend the present work by investigating the effect of faults on the optimized PSS, applying new metaheuristic optimization algorithms in hope to find new PSS parameters, which may result in better system eigenvalues or developing new PSS structures being more suitable to enhance power system stability.

Bibliography

[1] P. Kundur, N. J. Balu, and M. G. Lauby, *Power system stability and control*, McGraw-hill, 1994.

[2] H. Saadat, *Power system analysis*, 3rd edition, PSA Publishing LLC, 2011.

[3] J. Machowski, Z. Lubosny, J. W. Bialek and J. R. Bumby, *Power system dynamics: stability and control*, 3rd edition, John Wiley & Sons, 2020.

[4] *Power system*, Accessed on: July 13, 2021. [Online] Available at: https://circuitglobe.com/power-system.html

[5] T. K. Nagsarkar, M. S. Sukhija, *Power system analysis*, 2nd edition, Oxford University Press, USA, 2014.

[6] I. Ellouze. *Etude de la stabilité et de la stabilisation des systèmes à retard et des systèmes impulsifs*. Université Paul Verlaine - Metz; Université de Sfax, 2010. Français.

[7] *Synchronous Generator Working Principle*, Accessed on: July 14, 2021. [Online] Available at: https://www.elprocus.com/synchronous-generator-construction-and-working/

[8] Yurika, Suwarno, G. H. M. Sianipar and J. Naiborhu, *Modelling of Synchronous Generator for Transient Stability in Power System*, 2019 2nd International Conference on High Voltage Engineering and Power Systems (ICHVEPS), 2020.

[9] *ECE 310 – PowerWorld*, Accessed on: July 14, 2021. [Online] Available at: https://www.powerworld.com/files/D02SynchronousMachines.pdf

[10] P. W. Sauer and M. A. Pai, J. H. Chow, *Power System Dynamics and Stability: With Synchrophasor Measurement and Power System Toolbox*, 2nd edition, Wiley, 2017.

[11] K. R. Padiyar, *Power System Dynamics: Stability and Control*, 2nd edition, John Wiley New York 1996.

[12] IEEE Committee Report, *Computer representation of excitation systems*, IEEE Transactions on Power Apparatus and Systems, vol. PAS-87, no. 6, pp. 1460 – 1464, 1968.

[13] A. S. Abdelhay and P. M. Om, *Power System Stability: Modelling, Analysis and Control*, the Institution of Engineering and Technology, 2015

[14] I. Dincer, M. F. Ezzat, *Comprehensive Energy Systems*, Elsevie, 2018.

[15] A. Arif, Z. Wang, J. Wang, B. Mather, H. Bashualdo and D. Zhao, *Load Modeling-A Review*, IEEE Transactions on Smart Grid, vol. 9, no. 6, pp. 5986 – 5999, 2018.

[16] E. V. Larsen, D. A. Swann, *Applying Power System Stabilizers Part I: General Concept*, IEEE Transactions on Power Apparatus and Systems, vol. PAS-100, no. 6, pp. 3017 – 3024, 1981.

[17] G. S. Vassell, *Northeast blackout of 1965*, IEEE Power Engineering Review, pp. 4–8, Jan. 1991.

[18] P. Kundur et al., *Definition and classification of power system stability IEEE/CIGRE joint task force on stability terms and definitions*, IEEE Transactions on Power Systems, vol. 19, no. 3, pp. 1387 – 1401, 2004.

[19] G. B. Jadhav, C. B. Bangal, and S. Kanungo. *Review of Transient Stability Enhancement in Multi-Machine Power System by using Various Types of PSS & FACT's Devices*, International Journal of Electrical Electronics & Computer Science Engineering, vol. 4, no. 6, E-ISSN : 2348-2273, P-ISSN : 2454-1222, 2017.

[20] *Classification of power system stability*, Accessed on: July 20, 2021. [Online] Available at: https://top10electrical.blogspot.com/2015/05/classification-of-power-system-stability.html

[21] W. Fang, P. Wei, Z. Du, *Reduced-order method for computing critical eigenvalues in ultra-large-scale power systems*, IET Generation, Transmission & Distribution, ISSN 1751-8687, 2010.

[22] *Assessing the Impact of DFIG Synthetic Inertia Provision on Power System Small-Signal Stability*, Accessed on: July 22, 2021. [Online] Available at: https://www.mdpi.com/1996-1073/12/18/3440/htm

[23] M. Clerc, *Particle Swarm Optimization*, John Wiley & Sons, 2010.

[24] P. Agnihotri, J. K. Dwivedi and V. M. Mishra, *Stabilization of Power System Using Artificial Intelligence Based System*, International Journal of Advance Research, Ideas and Innovations in Technology, vol. 3, no. 1, pp. 966 – 973, 2017.

[25] A. E. Hassanien, T.H. Kim, J. Kacprzyk, A. I. Awad, *Bio-inspiring Cyber Security and Cloud Services: Trends and Innovations*, Springer, 2014.

[26] R. Poli, J. Kennedy, T. Blackwell, *Particle swarm optimization An overview*, Springer Science & Business Media, LLC 2007.

[27] H. Shayeghi, A. Safari, H. A. Shayanfar, *Multi-machine Power System Stabilizers Design Using PSO Algorithm*, International Journal of Electrical Power and Energy Systems Engineering, 2008.

[28] M. Eslami, H. Shareef, M. Azah and S. P. Ghoshal, *Tuning of power system stabilizers using particle swarm optimization with passive congregation*, International Journal of the Physical Sciences, vol. 5 no. 17, pp. 2574 – 2589, 2010.

[29] V. Keumarsi, M. Simab, G. Shahgholian, *An integrated approach for optimal placement and tuning of power system stabilizer in multi-machine systems*, International Journal of Electrical Power & Energy Systems, vol. 63, pp. 132-139, 2014.